Journal of Hydrology: Regional Studies 49 (2023) 101487

Contents lists available at ScienceDirect

Journal of Hydrology: Regional Studies

journal homepage: www.elsevier.com/locate/ejrh

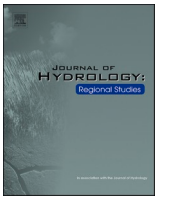

Seasonal streamflow forecasting in South America's largest rivers

Ingrid Petry [a,*,1], Fernando Mainardi Fan [a], Vinicius Alencar Siqueira [a], Walter Collishonn [a], Rodrigo Cauduro Dias de Paiva [a], Erik Quedi [a], Cléber Henrique de Araújo Gama [a], Reinaldo Silveira [b], Camila Freitas [c], Cassia Silmara Aver Paranhos [c]

[a] Hydraulic Research Institute, Federal University of Rio Grande do Sul, Porto Alegre, Brazil
[b] SIMEPAR, Curitiba, Brazil
[c] COPEL, Curitiba, Brazil

ARTICLE INFO

Keywords:
Seasonal streamflow forecast
Bias correction
South America

ABSTRACT

Study region: South America large basins (>5000 km^2)
Study focus: This work represents a first assessment of seasonal streamflow forecasts in South America based on a continental-scale application of a large scale hydrologic-hydrodynamic model and ECMWF's seasonal forecasting system precipitation forecasts (SEAS5-SSF) with bias correction. Seasonal streamflow forecasts were evaluated against a reference model run. Forecast skill was estimated relative to the Ensemble Streamflow Prediction (ESP) method.
New hydrological insights: We observed that bias correction was essential to obtain positive skill of SEAS5-SSF over ESP, which remained a hard to beat benchmark, especially in regions with high seasonality, and highly dependent on initial conditions. SEAS5-SSF skill was found to be dependent on initialization month, basin and lead time. Rivers where the skill is higher were Amazon, Araguaia, Tocantins and Paraná.

1. Introduction

Seasonal streamflow forecasts (SSF) provide estimates of river discharges up to 6–9 months in advance. This information finds special demand where long term hydrological planning plays an important role. For instance, it can be used to improve the efficiency of reservoir operation (Lee et al., 2020; Peñuela et al., 2020), to help water allocation decisions (Chiew et al., 2003; Crochemore et al., 2021; Kaune et al., 2020), to create flood mitigation strategies (Kompor et al., 2020; Paiva et al., 2013) and as a drought management tool (Carrão et al., 2018; Sutanto et al., 2020).

A Hydrological Ensemble Prediction Systems (H-EPS) is considered the state of the art of rivers streamflow prediction (Troin et al., 2021). It typically combines hydrological models with ensemble Quantitative Precipitation Forecasts (QPF), resulting in probabilistic estimates of future streamflow (Cloke and Pappenberger, 2009), and the QPF are the source of information on the future water input. This method has been widely used in different works (Buizza et al., 2005; De Paiva et al., 2020; Delorit et al., 2017; Demirel et al., 2015; Hersbach, 2000; Van Dijk et al., 2013; Van Hateren et al., 2019).

* Corresponding author.
E-mail address: ingrid.petry@ufrgs.bra (I. Petry).
[1] Address: Rua Ramiro Barcelos, 1920, apto 32, CEP: 90035-002 Porto Alegre, Brazil.

https://doi.org/10.1016/j.ejrh.2023.101487
Received 9 August 2022; Received in revised form 20 July 2023; Accepted 27 July 2023
Available online 3 August 2023

In the seasonal hydrological prediction scale, the traditional approach known as Ensemble Streamflow Prediction (ESP) produces ensemble forecasts by using a hydrological model with appropriated initial conditions forced with future precipitation scenarios resampled from historical observations (Day, 1985). In other words, the method project historical observation into the seasonal future as the ensemble precipitation forecasts, resulting in a tough to beat streamflow forecast benchmark (Harrigan et al., 2018; Peñuela et al., 2020), therefore being an adequate comparison to evaluate forecasts skill (Pappenberger et al., 2015; Yuan, 2016; Yuan et al., 2015).

One of the major sources of streamflow forecasts predictability is the rainfall forecast. This is especially true for tropical regions, where the snowfall plays a less important role (Fan et al., 2015). However, rainfall forecasts are strongly dependent on its initial conditions due to the chaotic nature of the atmosphere (Lorenz, 1993), turning precipitation forecasts also a major source of SSF uncertainty. The use of ensembles instead of deterministic precipitation data was one of the advances developed to quantify uncertainty of the forecast (Buizza et al., 2005; WMO, 2008), besides the forecasts remaining systematic errors inherited from the meteorological model (Crochemore et al., 2016; Pechlivanidis et al., 2020).

In addition to Lorenz, Shukla (1998) observed that rainfall and tropical atmosphere large scale seasonal circulation are almost completely determined by the sea surface temperature (SST) conditions. Therefore, the precipitation could be better predicted not only considering the atmospheric initial conditions that produce useful forecasts up to 1 month, but also considering SST as a determining factor. This observation influenced meteorological centers to invest in improving the ability of models to predict large-scale climate phenomena, such as the El Niño Southern Oscillation (ENSO), a phenomenon featured by SST anomalies and one of the major sources of seasonal predictability in South America (Weisheimer et al., 2020). In 2019, ECMWF published the ECMWF fifth generation seasonal forecasting system (SEAS5) (Johnson et al., 2019a). ECMWF is among the best models capable of predicting ENSO phenomena (Barnston et al., 2012; Johnson et al., 2019a), and with both retrospective and operational forecasts available. SEAS5 data were found to have significant biases (Gubler et al., 2020; Wang et al., 2019) and the use of raw data is not encouraged (Wang et al., 2019).

One can find in the literature various works that investigate monthly to seasonal streamflow forecasts at basin scales (Collischonn et al., 2005; De Paiva et al., 2020; Delorit et al., 2017; Demirel et al., 2015; Kompor et al., 2020; Mahanama et al., 2012; Peñuela et al., 2020; Tucci et al., 2003; Van Hateren et al., 2019). These works raised important conclusions at the basin level, ranging from 1000 to 1.3 M km^2. However, at a continental level, generally they represent fragmented information and do not allow a comprehensive and comparative evaluation of forecasts performance. Hydrological events are not necessarily originated outside the catchment borders (Emerton et al., 2016) and may impact multiple basins and sites (Fleischmann et al., 2020). Thus, it is valuable to have a multi-basin modelling approach to give profound understanding on the dynamics of hydrological processes and to assess the forecasts spatial consistency (Pechlivanidis and Arheimer, 2015). Global or continental scale forecasts can contribute to the spatial understanding of hydrological predictabilities while providing information for regions where no other forecasting system exists, due to its ability to cover different geographic and climatic regions (Emerton et al., 2018; Gupta et al., 2014).

Scientific and technological advances, as well as the integration of research communities, are required to produce large to global scale forecasts (EMERTON et al., 2016). In Yossef et al. (2013). published a study on the skill of global seasonal streamflow forecasting system. More recently, one of the first attempts in producing and providing seasonal hydro-meteorological forecast products openly at global scale was released, the GloFAS-Seasonal V1.0 (Emerton et al., 2018). However, global-scale forecasts still face many challenges, such as the lack of available data in the temporal and spatial scales required for application, the communication of forecasts to end users across the globe (Emerton et al., 2016) and the limited ability of global models to simulate streamflow at local scales (Archfield et al., 2015). Especially at the continental level, most studies in the topic of seasonal streamflow forecast were developed over Europe, for instance Greuell et al. (2019), Pechlivanidis et al. (2020), Sutanto et al. (2020) and EFAS-Seasonal (Arnal et al., 2018); and on a country scale with continental dimensions, there are some studies in the United States of America (Koster et al., 2010; Mahanama et al., 2012; Najafi et al., 2015) and China (Liu et al., 2021). One recent work for South America presents a seasonal runoff forecast with a simplified approach for the continent (Greuell and Hutjes, 2023).

In South America (SA), Siqueira et al. (Siqueira et al., 2018) developed a continental-scale version of the MGB (*Modelo de Grandes Bacias*) hydrologic-hydrodynamic model (Pontes et al., 2017), which has been applied and consolidated in large tropical basins in South America (Brêda et al., 2020; Collischonn et al., 2007, 2005; Fan et al., 2016; Fleischmann et al., 2020; Lopes et al., 2018; Petry et al., 2022; Pontes et al., 2017; Quedi and Fan, 2020; Siqueira et al., 2016). Expanding regional models to continental scale is considered a viable alternative to overcome some global scale models limitations, bridging gaps between the modelling approach and the better use of local expert knowledge and country-specific datasets (Siqueira et al., 2018). The South American MGB has already been used in medium-range streamflow prediction, through the forecast module that runs Ensemble Streamflow Predictions (ESP) and Hydrological Ensemble Prediction Systems (H-EPS) (Siqueira et al., 2021, 2020).

Given this scenario and motivated by the recent advances of continental hydro-meteorological modelling in South America, this work aimed to verify the following hypothesis: (i) seven months lead time seasonal precipitation forecasts, when used to feed a continental hydrological-hydrodynamic model, can outperform the ESP benchmark forecasts in South America; (ii) the performance of continental forecasts varies, particularly with respect to precipitation, the seasonal changes in streamflow, and the characteristics of the basin; and (iii) bias correction of precipitation forecast improves the intended result. Besides, we analyzed the performance of an operational seasonal streamflow forecast issued in the South American context.

For this, we will assess the current performance and skill of seasonal streamflow forecasts produced with continental application of a regional hydrodynamic-hydrological model (MGB-SA) and SEAS5 precipitation forecasts (SEAS5-SSF) with bias correciton. With MGB-SA, results are issued for natural flows of rivers in large basins (>5000 km^2) with daily time steps and are analyzed at monthly time steps. The skill assessed was the "theoretical skill", the added value from the H-EPS by neglecting the errors in the hydrological models by comparing results with the ESP benchmark from the same hydrological model. Streamflow performance thresholds

representing low flows are adopted considering that a few months in advance can benefit a variety of sectors in the continent, by allowing sufficient lead time for drought preparedness and mitigation efforts (Carrão et al., 2018).

2. Methodology

The methods adopted in this study are summarized in the flowchart of Fig. 2. Seasonal streamflow forecasts are obtained by forcing the MGB-SA model with raw and bias-corrected SEAS5 predicted precipitation. Forecast performance is evaluated against a reference MGB-SA run (MSWEP precipitation as input) by using deterministic and probabilistic metrics and the Ensemble Streamflow Prediction approach (ESP) is used as a benchmark to evaluate the added skill of SEAS5-based streamflow forecasts (SEAS5-SSF). The streamflow forecast analysis was from 2007 to 2016 for the hindcast data and from 2017 to 2021 for precipitation forecast, totalizing 14 years streamflow forecast results. These methods are further detailed in the following sections.

2.1. Study area: South America (SA)

Situated between the Atlantic and Pacific Oceans, South America (SA) is a continent with an area of approximately 17.8 million square kilometers and 90% of its lands are in the Southern Hemisphere. The continent's outline is drawn by the Andes Mountain Range, the North-Amazonian residual plateaus and plateaus and mountains of the Atlantic-East-Southeast. Among them, there are lowland areas where the three main hydrographic basins in South America are located: Amazon, Orinoco and La Plata. The elevation

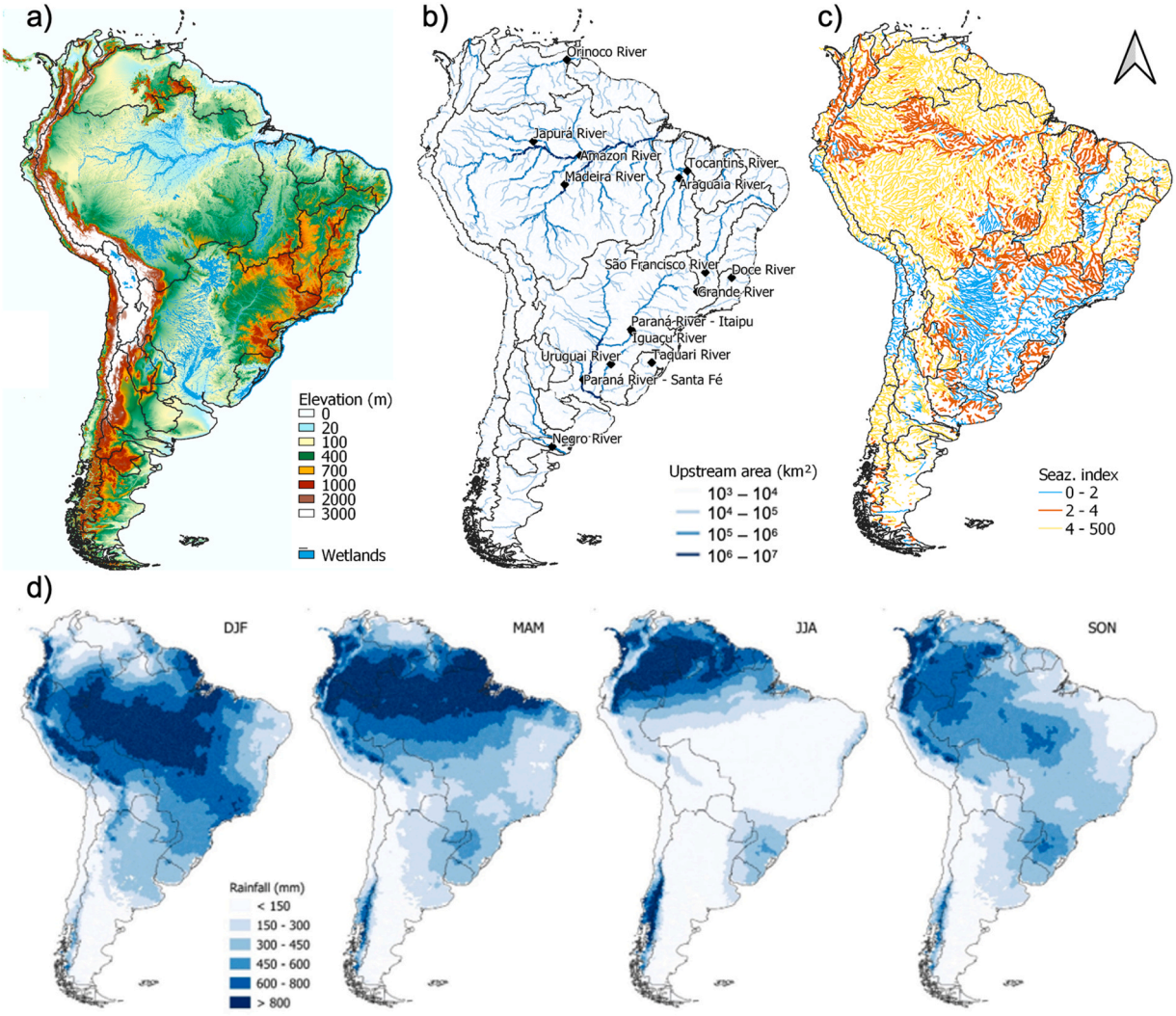

Fig. 1. a) South America elevation map, wetlands and countries' borders; b) SA river's upstream area, important river sites of SA and great SA basins delimitation; c) Rate between the maximum and the minimum monthly Q95; and d) average annual precipitation in South America according to the season, extracted from the MSWEP database (Beck et al., 2017).

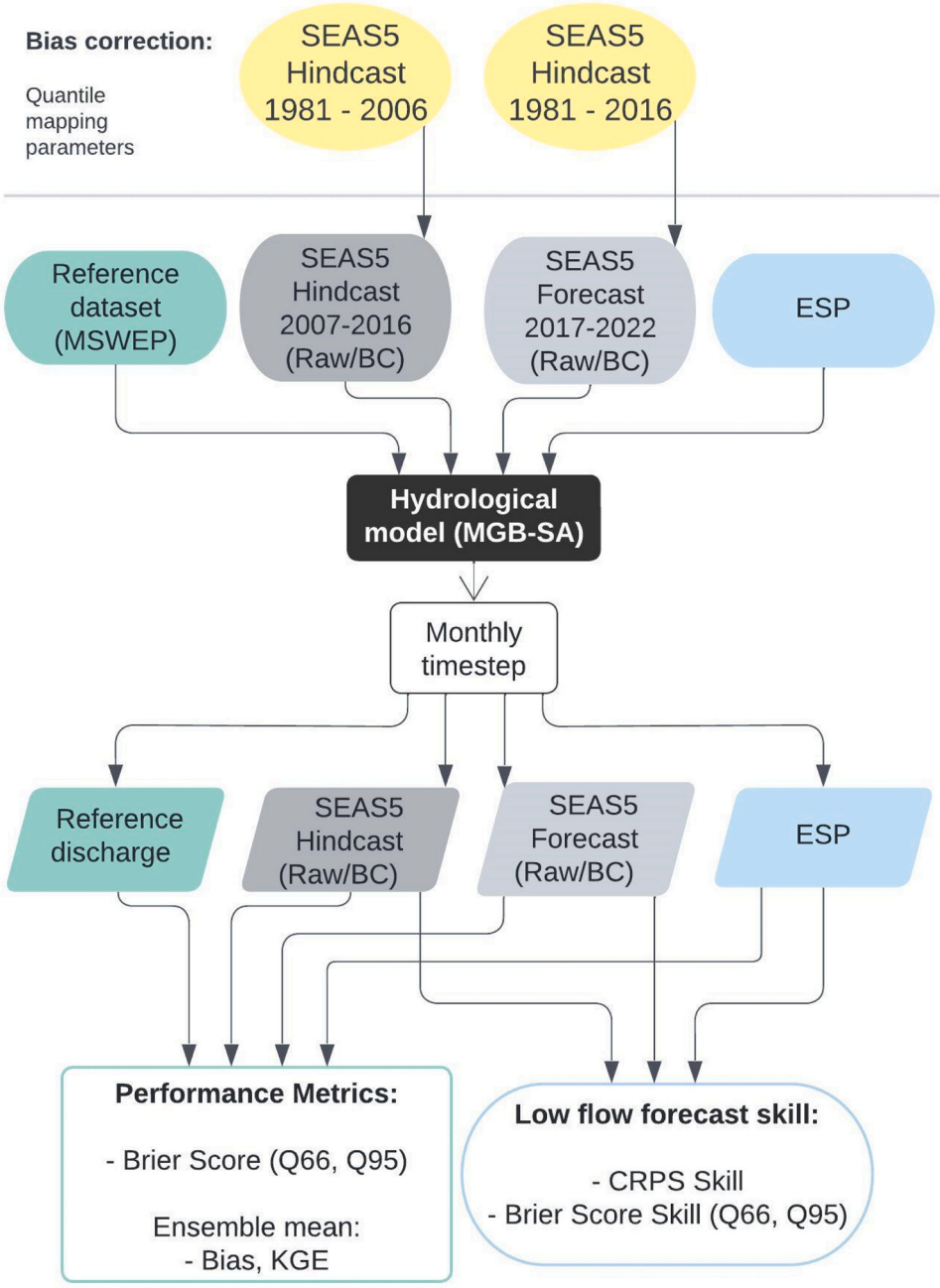

Fig. 2. Methodology flowchart, in grey the SEAS5-SSF elements, green the reference discharge and blue ESP.

map of South America and its humid areas can be seen in Fig. 1a. Fig. 1b shows rivers' upstream area and other important rivers of South America, such as Araguaia, Tocantins, Paraná, Uruguay and São Francisco.

Most of the territory (~80%) is under the influence of a tropical climate, typically characterized by a rainier (and hotter) season and a drier season. However, the precipitation regime isn't homogeneous. Precipitation regimes in SA exhibit large spatial variability due to its wide meridional extent (12ºN-55ºS), complex topography (e.g., Andes), particular vegetation features (Amazon rainforest) and influence of the adjacent Atlantic and Pacific oceans (Ferreira and Reboita, 2022; Garreaud, 2009). Seasonal mean precipitation is presented in Fig. 1d. During the austral summer (DJF), the maximum precipitations are concentrated in the central-west region of Brazil, migrating to the north of the equator during the austral winter (JJA). The North of SA is a region of abundant precipitation throughout the year, while the South of SA is much drier. Another exception is the southeastern SA, where one can verify precipitations all over the year.

Fig. 1c presents the rate between the maximum and the minimum monthly Q95 (streamflow that is exceeded 5% of the time). Greater values indicate stronger seasonal patterns of streamflow throughout the year.

2.2. MGB-SA model

MGB-SA is a continental-scale version of the MGB model (*Modelo de Grandes Bacias*) developed specifically for the South America region (Siqueira et al., 2018). The model was selected as the main tool for continental hydrological-hydrodynamic modelling from its capacity of representing the continent main hydrological process, popularity and added value in producing prognostic results in prior researches in the continent (Brêda et al., 2020; Fan et al., 2014; Fan et al., 2016; Fleischmann et al., 2019, 2020; Petry et al., 2021; Quedi and Fan, 2020; Siqueira et al., 2021, 2020, 2016).

It is a conceptual, semi-distributed hydrologic-hydrodynamic model that discretizes the spatial domain into unit-catchments and further into Hydrological Response Units (HRUs), which are categorized by combinations of land use and soil type information (Paiva et al., 2013). Soil is depicted as a bucket model with a single layer. Water budget and energy balance are computed at the HRU level with a daily time step, and the HRU values are interpolated to each unit-catchment centroid. Each unit-catchment has a unique river reach, where the river routing processes are performed.

The model uses the Penman-Monteith equation to calculate evapotranspiration and produces surface runoff using the variable contribution area concept following the Arno model. Groundwater and subsurface flows are computed using linear and nonlinear functions according to water availability in the soil layer. Runoff from each component is propagated to the stream network using linear reservoirs. The MGB-IPH model can be used with different flow routing methods, including the Muskingum-Cunge method, a one-dimensional full hydrodynamic method, or the local inertial method (Pontes et al., 2015). The routing structure of MGB is similar to that described by Yamazaki et al., (2013, 2011). In addition, the model accounts for evaporation in floodplains and infiltration from flooded areas to the unsaturated soil.

We used state of art daily precipitation data from (i) the Multi-Source Weighted Ensemble Precipitation v1.1 (MSWEP) (Beck et al., 2017) until the year of 2014 and (ii) the Integrated Multi-satellite Retrievals for GPM – Global Precipitation Measurement (GPM-I-MERG, Version 06) final run from 2015 to 2021, following the same modelling datasets as (Alves et al., 2022; Petry et al., 2022). MSWEP (v1.1) is a gridded database with 0.25° spatial resolution and global coverage that combines precipitation from satellite, reanalysis and in situ gauges. IMERG combines data from the GPM satellite constellation and provides gridded precipitation estimates with spatial resolution of 0.1° for the entire globe between latitudes 60°N and 60°S (Skofronick-Jackson et al., 2017). The GPM data was adjusted to the MSWEP database using the parametric quantile method (Piani et al., 2010), which fits a gamma distribution to the cumulative distribution of both precipitation databases. A bias correction was applied to reduce systematic differences in relation to MSWEP, as the MGB-SA was calibrated with the MSWEP database.

Climate data used to calculate evapotranspiration (temperature, sunshine, relative humidity, pressure and wind speed) were the Climate Research Unit (CRU) v.2 monthly means, which are ground-based, relative to the 1961–1990 period and are provided at a 10' resolution (New et al., 2002). For each simulated/forecasted day we used the monthly average of the respective month. MSWEP and CRU data were interpolated to the MGB-SA unit-catchments by using the inverse-distance-weighted and nearest neighbor methods, respectively. Table 1 present all the datasets that were used on MGB-SA.

The MGB-SA was manually calibrated with hundreds of in situ observations upstream to downstream of the rivers in large basins (>1000 km^2) in SA. For the period of (1990 – 2010) the model showed satisfactory performance (KGE > 0.6 in more than 70% of the gauges evaluated) and an improvement of around 20 days regarding flood timing in large rivers (e.g., Amazon, Paraguay) when

Table 1
Description of the datasets of MGB-SA and SSF experiments.

Information	Data description	Spatial resolution	Reference
Digital elevation model (DEM)	Bare-Earth SRTM v 1.0 DEM	Resampled from 3″ to 15″ (~90 m to ~500 m)	O'Loughlin et al. (2016)
Flow directions map	Global HydroSHEDS Flow Direction map, 15″	15″	Lehner and Döll (2004)
Meteorological forcing	Climatological monthly averages from Climate Research Unit (CRU Dataset v. 2.0)	-	New et al. (2002)
	Global Multi-Source Weighted Ensemble Precipitation v 1.1 (MSWEP)	0.25 degrees	0.25 degrees
Streamflow ground data	In situ observations - ANA (Brasil), Naturalized flows of reservoirs (ONS - Brasil), INA (Argentina), IDEAM (Colombia), DGA (Chile), SENAMHI (Peru and Bolivia), ORE-HyBAM (International), Global Runoff Data Centre (International)	in situ	-
Soil data	Map of Hydrological Response Units in South America	-	Fan et al. (2015)
Hydrographic regions	Brazilian hydrographic divisions (ANA): http://metadados.ana.gov.br/geonetwork/srv/ pt/main.home Mapa Aquastat: http://www.fao.org/geonetwork/srv/en/metadata.show?id= 37174	-	-
Width / Depth of full river channel	Geomorphological relationships from regional studies, Amazonia, Prata, Lagoa dos Patos Basin (RS) Global bankfull width and depth database (other locations)	-	Andreadis et al. (2013), Paiva et al. (2013), Pontes (2016), Lopes (2017), Beighley and Gummadi (2011)

compared to individual global models (Siqueira et al., 2018). Regarding the stations with poorer KGE results, most of these stations are in regions with a semi-arid climate, or close to the Andes where the orography is quite complex and rainfall estimates have greater uncertainties, as Fig. 3 shows. In some areas further south of the continent, there are also limitations in rivers influenced by melting snow from the Andes, since the model does not have the capacity to simulate such processes.

When considering factors that may have influenced the performance of the MGB model during the calibration phase, it is pertinent to note that water withdrawals are not incorporated into the model's simulations. Despite this, significant impacts on observed discharges are not usually expected at most gauge stations, especially those with an upstream drainage area exceeding 10,000 km^2. However, it's likely that model performance was somewhat diminished in gauges located within drier regions due to such human-induced influences. Reservoir operations represent another factor that can markedly affect observed flows, and this remains true even for substantial rivers. We want to highlight that during the calibration process, we intentionally removed those gauge stations that exhibited a high degree of regulation due to reservoirs. This was accomplished through careful visual inspection. Moreover, we

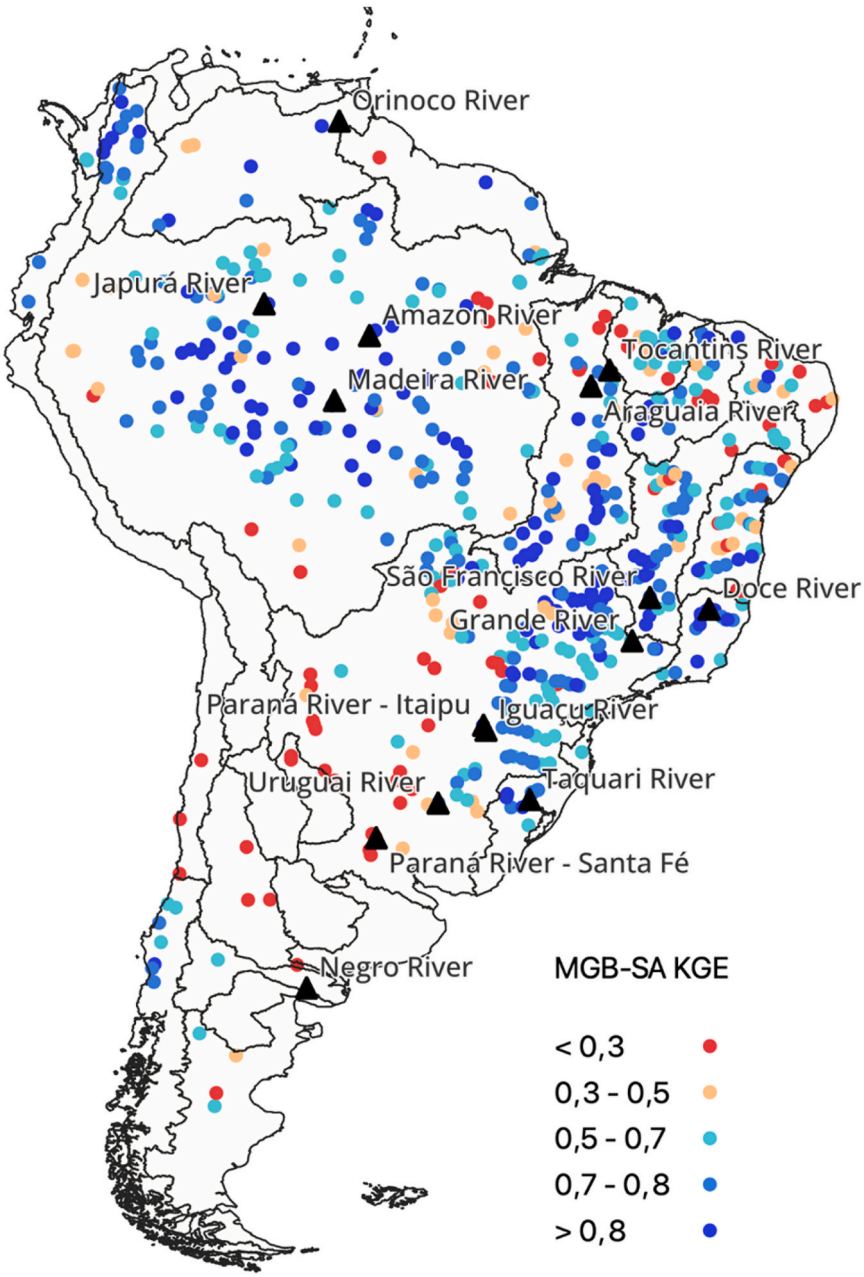

Fig. 3. MGB-SA KGE of in situ gauges for the simulation period (1990–2010).

made use of naturalized flows at reservoir locations, which were kindly provided by the Brazilian National Electric System Operator (ONS), as additional data for refining our model. For a more thorough insight into the model's configuration, we suggest reviewing the study conducted by Siqueira et al. (2018).

2.3. Precipitation hindcasts and forecasts

We used the fifth generation of the ECMWF seasonal forecasting system (SEAS5) (Johnson et al., 2019a) as the source of predicted precipitation. The data is made available by the Copernicus Climate Change Service (C3S), a platform that provides unrestricted access to forecast data to its users (Buontempo et al., 2020).

The SEAS5 system has a forecast horizon of 215 days (~7 months), spatial resolution of approximately 36 km (we used 100 km) and temporal resolution of 24-h accumulation interval. Seasonal forecasts are issued on the first day of each month, for a given year (Johnson et al., 2019a). ECMWF's SEAS5 provides both Hindcasts (retrospective forecasts for multiple years in the past), and real-time operational Forecasts. Real-time Forecasts have 51 ensemble members for which data is available from 2017 onwards and we obtained real-time precipitation forecasts from the C3S for the period between Jan/2017–Dec/2021. In turn, Hindcasts are available from 1981 to 2016 and are produced with a forecast system that is as close as possible to that used operationally, having a reduced ensemble of 25 members. As Hindcasts are consistent with the operational forecasts and are available for a longer period (35 years), they were used to correcting biases for both evaluated periods (2007–2016 and 2017–2021, see section 3.2.3).

2.3.1. Bias correction of SEAS5 predicted precipitation

Meteorological forecasts are found to have systematic errors (bias) inherited from meteorological models (Crochemore et al., 2016; Kim et al., 2012; Yuan et al., 2015), and the SEAS5 precipitation product is no different (Gubler et al., 2020; Pechlivanidis et al., 2020; Wang et al., 2019). To reduce existing bias in SEAS5, the widely used Quantile Mapping method (Bárdossy and Pegram, 2011) was applied as follows:

$$Z_C(x,t) = F_O^{-1}(F_R(Z_R(x,t),x),x) \quad (1)$$

where Zc is the bias-corrected SEAS5 precipitation at location x and day t simulated by ECMWF, Fo^{-1} is the inverse form of the cumulative distribution function (CDF) of the observed precipitation, Fr is the CDF of the SEAS5 raw precipitation and Zr is the raw precipitation at location x and day t.

Parametric gamma distributions were adjusted for hindcasts, forecasts and MSWEP precipitation estimates to apply the quantile mapping in each unit-catchments separately. To obtain the parameters of gamma distributions regarding the predicted precipitation, we created subsets of data by separating SEAS5 daily precipitation hindcasts of each month along the forecast horizon (7) and each forecast initialization month (12). All 25 ensemble members were considered to increase the sample size, assuming the equiprobability of the ensemble members from the SEAS5 description (Johnson et al., 2019b).

The corresponding MSWEP data of each forecast subset were then used to obtain the parameters of gamma distributions for observations. The data used to obtain SEAS5 raw precipitation parameters was the hindcast from 1981 to 2006 for the hindcast experiments and hindcast from 1981 to 2016 for the forecast experiments, a similar approach as used by Yuan et al. (2015). Fig. 4 presents a summary on the periods of precipitation Forecasts and Hindcasts used on bias correction and experiments analysis, as well as the observed precipitation used for model initialization and reference run. Bias correction was performed after the precipitation data (both observed and predicted) had been interpolated to the MGB-SA unit-catchment centroids using the inverse distance weighting method.

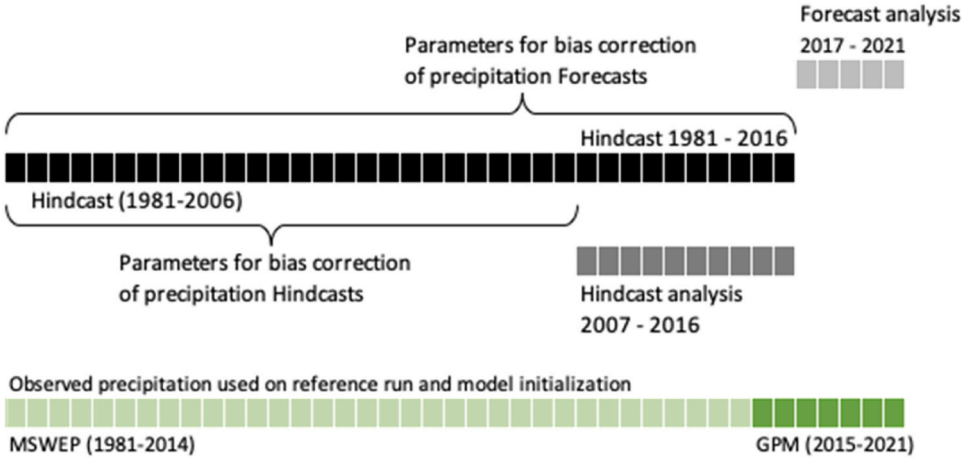

Fig. 4. Precipitation Forecasts and Hindcasts periods used on bias correction and experiments analysis.

2.4. Generation of seasonal streamflow forecasts

Seasonal streamflow forecasts were produced with the MGB-SA model by following the steps presented in Siqueira et al. (2020). First, a long-term simulation run was performed from 1980 to 2021 and model initial conditions (e.g., soil moisture content, volume of water in rivers and floodplains, etc.), were sequentially saved for the first day of each month along the forecast evaluation periods (between Jan/2007 and Dec/2021, considering both the hindcast and forecast evaluation periods). Next, raw and bias-corrected SEAS5 predictions were used to force the MGB-SA using the updated model states that were saved for each forecast/hindcast initialization day.

MSWEP v1.1 precipitation data and the climate data from the global CRU database used on the calibration period are the same used to initialize the model in the evaluation period of the Hindcasts (except for the last two years, 2015 and 2016, but the data used here were bias corrected). The data used to initialize the model for the Forecasts experiments were the GPM v6.

For the skill assessment of SEAS5-SSF, the ESP approach was used as a benchmark. The ESP builds meteorological forecast scenarios resampled from past observations and uses them as inputs to a hydrological model with updated initial conditions (Day, 1985; Wood and Lettenmaier, 2008). This method has been commonly used to assess the added skill of seasonal streamflow forecasts based on dynamic forecasting systems (Alfieri et al., 2014; Arnal et al., 2018). To generate the predicted precipitation ensemble for the ESP benchmark, we resampled the historical rainfall data (MSWEP/GPM-IMERG) from all years between 1979 and 2020 for the same calendar date (i.e., same day and month) of the corresponding hindcast/forecast lead time, excluding the target year. This resulted in a precipitation ensemble composed of 41 members, which was then used as input to MGB-SA (with updated model states) to produce the ESP.

2.5. Streamflow forecast assessment

For the assessment, seasonal streamflow forecasts were averaged from daily to monthly time step. The performance metrics applied for the ensemble mean were, Relative Mean Error (bias) (%) and Kling–Gupta Efficiency (Gupta et al., 2009). For the ensemble, we calculated the continuous ranked probability score (CRPS) (Brown, 1974; Hersbach, 2000) in terms of skill and Brier Score (BS) for both performance value and skill (Brier, 1950).

The Kling–Gupta Efficiency (KGE) is a metric used in hydrology to summarize model performance:

$$KGE = 1 - \sqrt{(r-1)^2 + \left(\frac{\sigma_{sim}}{\sigma_{obs}} - 1\right)^2 + \left(\frac{\mu_{sim}}{\mu_{obs}} - 1\right)^2} \tag{2}$$

where r is the linear correlation between observations and simulations, σobs is the standard deviation in observations, σsim the standard deviation in simulations, μsim the streamflow simulation mean and μobs the observation mean. KGE ranges from -∞ to 1 and KGE = 1 indicates perfect agreement between simulations and observations.

The continuous ranked probability score (CRPS) is given as:

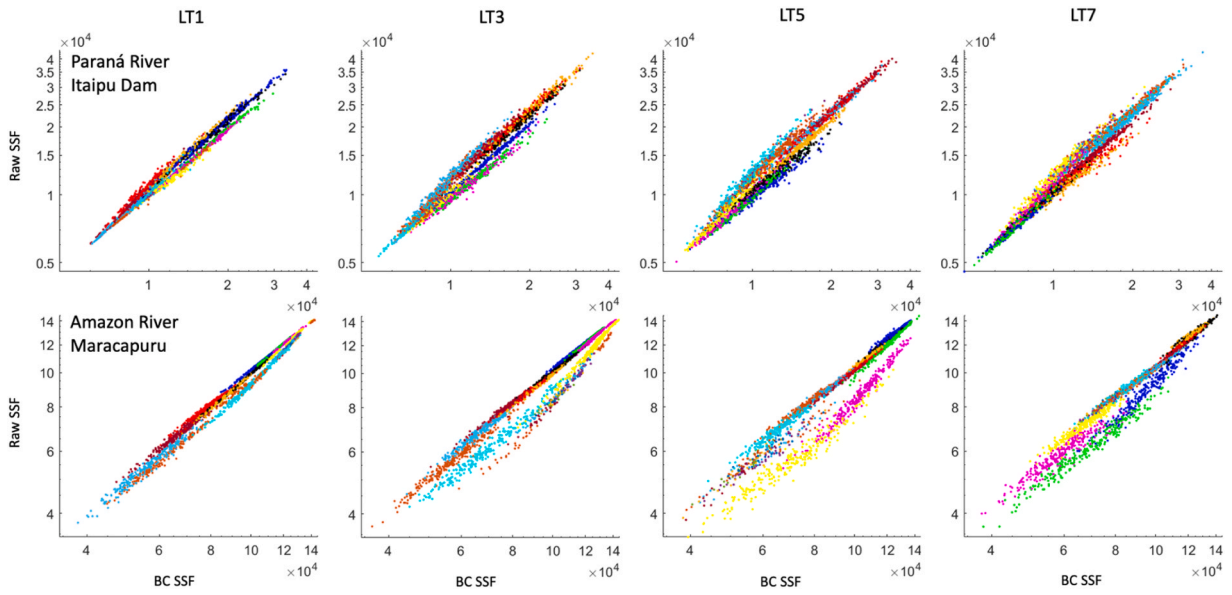

Fig. 5. Scatter plot of Hindcast SEAS5-SSF of raw and bias corrected (BC) precipitation.

$$CRPS_h = \frac{1}{N}\sum_{n=1}^{N}\int_{-\infty}^{+\infty}\left[F_P(QP_{h,n}) - F_O(QP_{h,n})\right]^2 dQP_{h,n} \quad (3)$$

where N is the total number of forecasts, Fp is the CDF of the ensemble forecast $QP_{h,n}$ and Fo is a step function that equals one for $QP_{h,n}$ values greater than or equal to the observation and zero otherwise. CRPS is calculated as a mean value by averaging the individual CRPS computed for each forecast n and a given lead time h.

The brier score (BS) is computed according to:

$$BS_h(L) = \frac{1}{N}\sum_{n=1}^{N}\left(F_{QP_{h,n}}(L) - \mathbf{1}(Q_{O_{h,n}} \le L)\right)^2 \quad (4)$$

where N is the total number of issued forecasts, h is the evaluated forecast horizon; L is a threshold that represents the occurrence of a hydrological event; $F_{Qph,n}$ is the proportion of the ensemble members that exceeds the evaluated threshold and $\mathbf{1}()$ is a function that equals one when the observed streamflow $Qo_{h,n}$ exceeds the evaluated threshold and is zero otherwise. Brier score indicates how good the forecast members are in the detection of a streamflow threshold. The chosen BS threshold aimed to assess the accuracy of the SEAS5-SSF in predicting a discharge lower than normal conditions and far below normal conditions. Thus, the threshold was the reference monthly streamflow that is exceeded 66% of the year (the lower tercile) and 95% of the time (Q_{95}), both for the past reference streamflow. These streamflows represent respectively low and very low flows (Liu et al., 2021).

H-EPS skill was calculated by evaluating both BS and CRPS of the SEAS5-SSF relative to that of the ESP benchmark:

$$BSS = 1 - \frac{BS_{SEAS5-SF}}{BS_{ESP}} \quad (5)$$

$$CRPSS = 1 - \frac{CRPS_{SEAS5-SF}}{CRPS_{ESP}} \quad (6)$$

Skill scores are calculated upon their previous performance (BS and CRPS). Their interpretation is very similar: results range from -∞ to 1, where positive values indicate that the SEAS5-SSF outperforms the ESP and vice-versa.

MSWEP streamflow simulations were used as reference simulations, since streamflow observations are not available to all the river reaches of South America. In this case, the predictability obtained is a theoretical skill, which may be greater than the actual skill, if observations were used. It occurs because the model and the precipitation are assumed to be perfect, which is not true. However, as in this work we aim to understand the potentials of seasonal streamflow forecast in South America from the MGB-SA model, this approach is acceptable. In the case of a forecast to a hydropower plant, a model bias correction would be applied considering the observed streamflow data.

2.6. Conducted experiments

To accomplish the objective of evaluating the performance and the skill of seasonal streamflow forecasts in the South American large rivers, the following experiments were conducted using the explained framework:

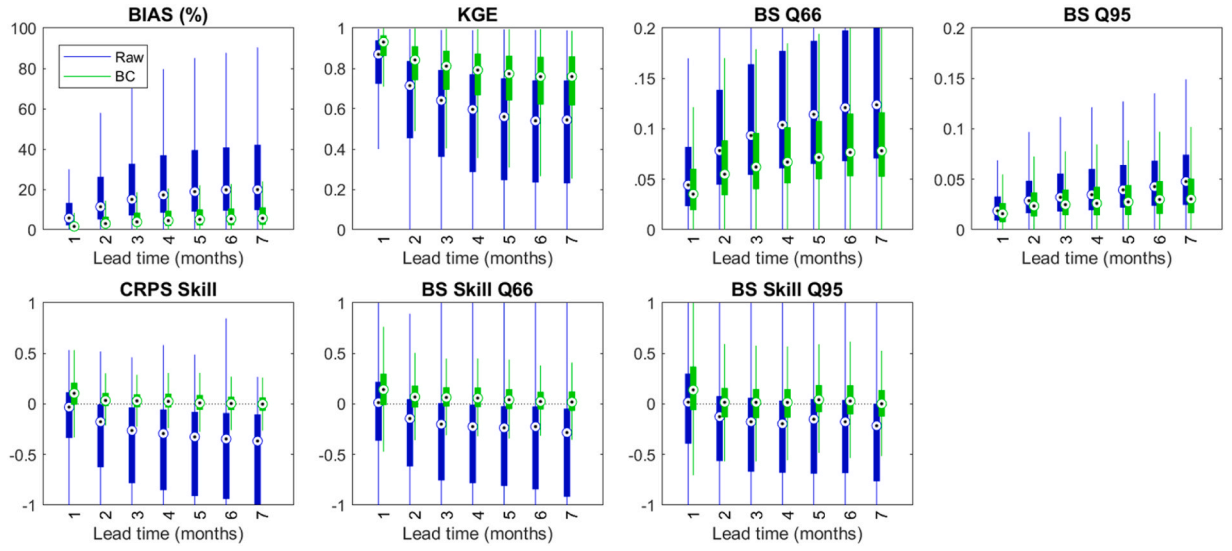

Fig. 6. SEAS5-SSF performance metrics for SA rivers with drainage area ≥ 5000 km^2, for the Hindcast experiments. Raw stands for no bias correction and BC for bias corrected precipitation streamflow forecast results.

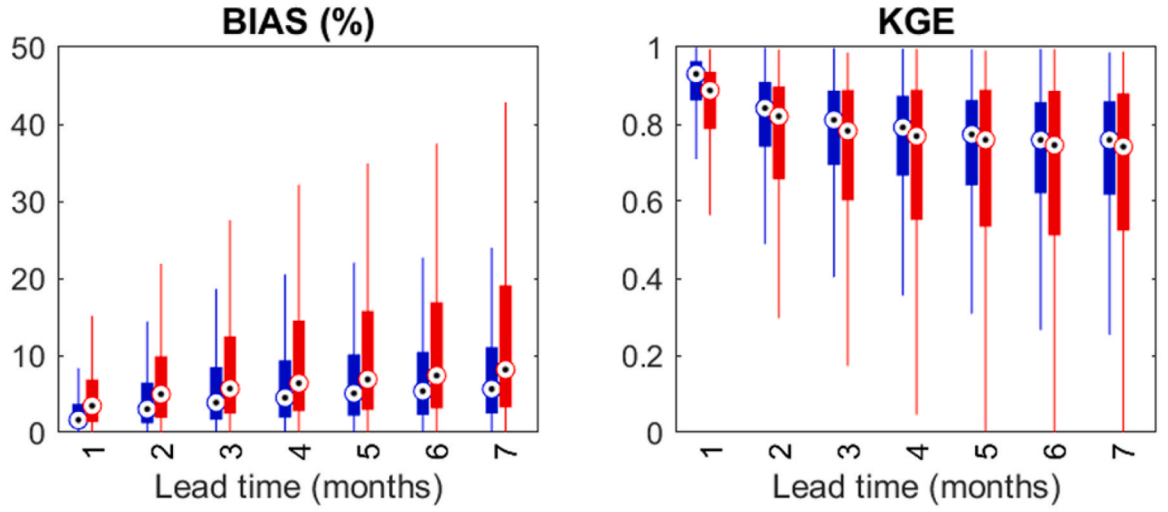

Fig. 7. Percentage bias and KGE for bias-corrected SEAS5-SSF according to lead time, considering rivers with drainage area $\geq 5000\ km^2$. Blue presents the Hindcast data results and Red the Forecast results.

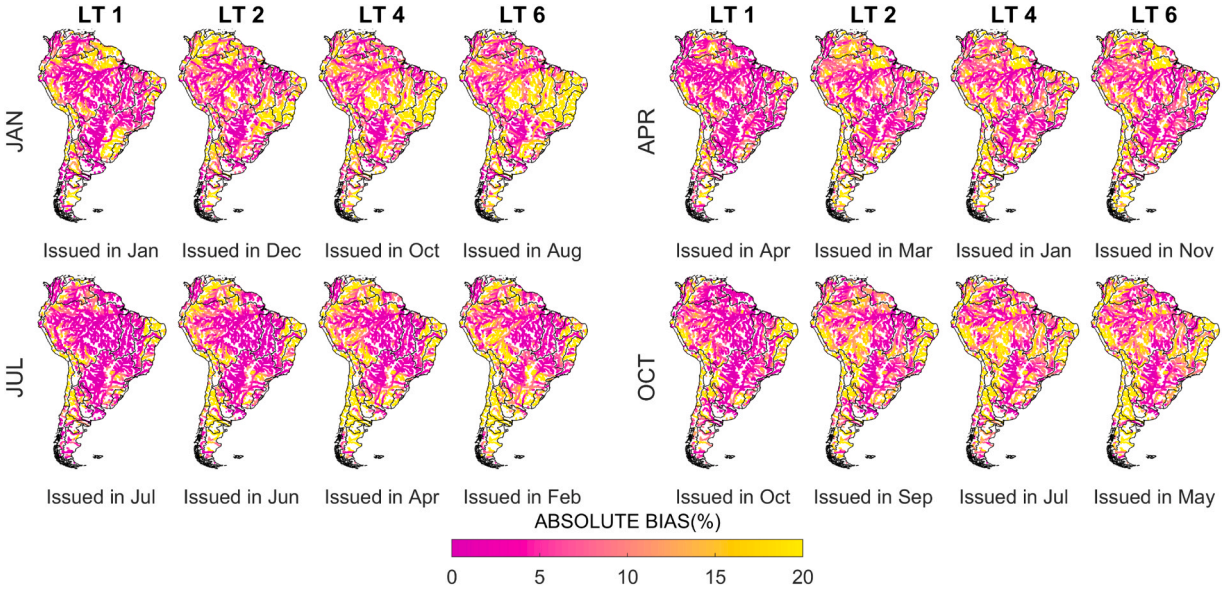

Fig. 8. Absolute Bias (%) in SEAS5-SSF (bias-corrected Hindcasts) according to season and lead time.

(i) A verification of the impact of the bias correction on seasonal streamflow forecasts.
(ii) An evaluation of the proposed forecasting framework based on SEAS5-SSF performance considering deterministic ensemble mean and full ensemble metrics, without comparing with the ESP results.
(iii) As Skill assessment comparing the forecasting framework based on SEAS5-SSF performance with the traditional ESP approach as a benchmark.
(iv) A visual more detailed analysis of the forecasting framework based on SEAS5-SSF with focus in a specific place during the 2020–2021 drought, to aid the kind of results generated.

3. Results

This section is divided in: (a) the impact of bias correction on seasonal streamflow forecast; (b) the SEAS5-SSF performance (ensemble mean and full ensemble); (c) SEAS5-SSF skill; and (d) detailed analysis of the SEAS5-SSF with focus on the Paraná Basin 2020–2021 drought.

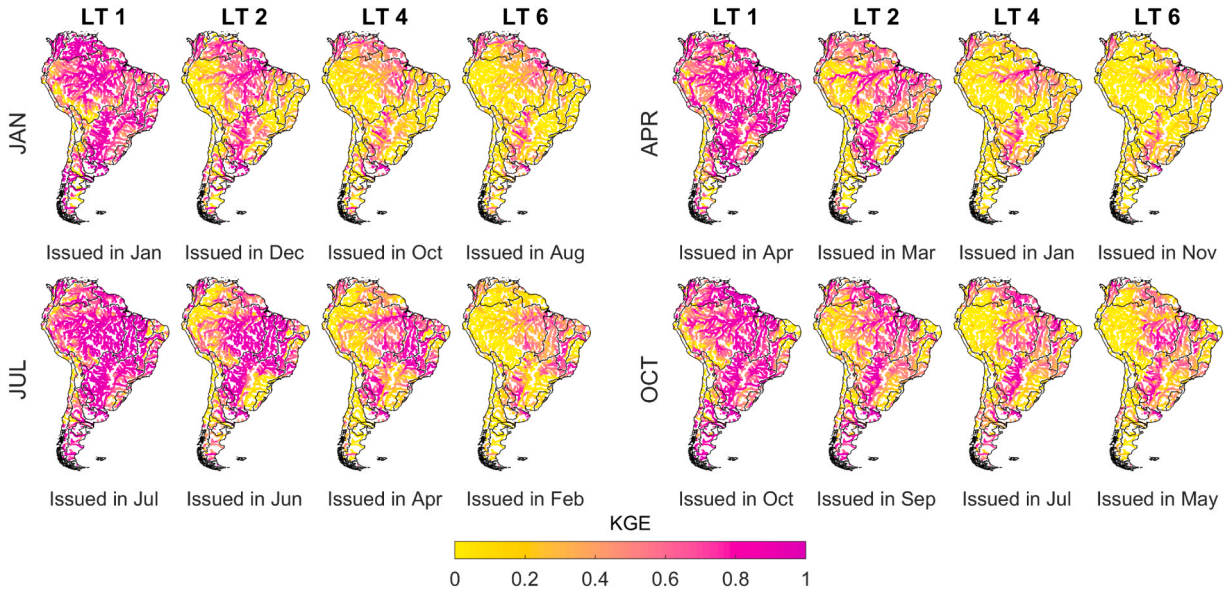

Fig. 9. KGE performance for SEAS5-SSF (bias-corrected Hindcasts) according to season and lead time over South American rivers.

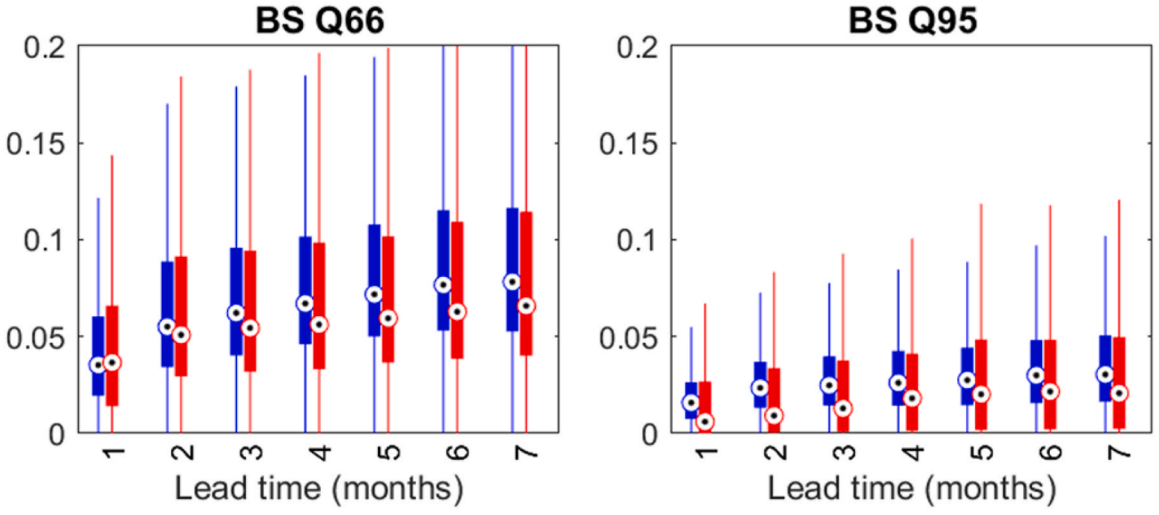

Fig. 10. Brier Score (Q66 and Q95) for bias-corrected SEAS5-SSF according to lead time, considering rivers with drainage area $\geq$ 5000 km^2. Blue presents the Hindcast data results and Red the Forecast results.

3.1. Impact of precipitation bias correction on seasonal streamflow forecast

Seasonal streamflow forecasts from raw and bias corrected precipitation Hindcasts are presented in Fig. 5 as scatter plots for the horizons 1, 3, 5 and 7 months. In the plots, each color represents a different target month and are presented for the Paraná River (Itaipu Dam) and Amazon River (Maracapuru). The figure shows the difference of streamflow values distribution according to the lead time and the target month, highlighting the importance on bias correcting the precipitation Hindcasts based on these two factors. Furthermore, we observe the reducing correlation of raw and bias corrected Hindcasts SEAS5-SSF with the increasing lead time. The same behavior was observed on precipitation Forecasts.

When bias correction is applied, the median performance of all evaluated metrics improves in the entire forecast horizon and the interquartile range of the boxplots is largely reduced. In particular, bias correction has a relevant impact on streamflow forecast skill, as CRPSS and BSS mostly change from negative to around zero or positive values. Fig. 6 shows boxplots of performance metrics (outliers suppressed) for bias-corrected and raw SEAS5-SSF, considering only river segments with drainage area greater than 5000 km^2 and results from the Hindcast experiments.

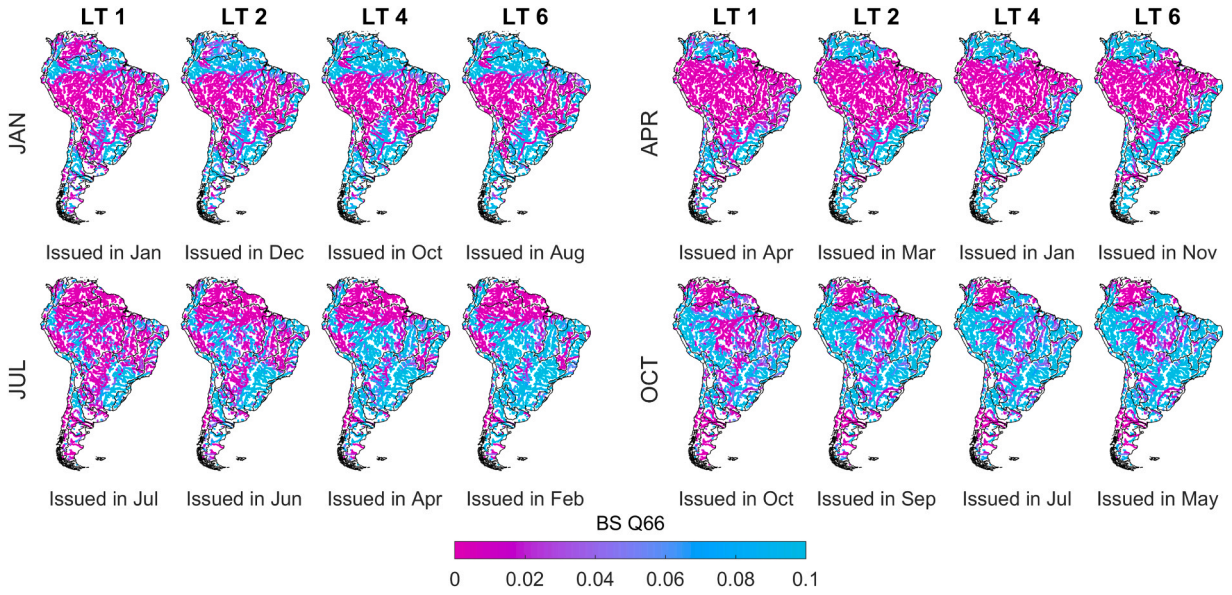

Fig. 11. Brier Score (Q66) for January, April, July and October for the lead time of one, two, four and six months (bias-corrected Hindcasts).

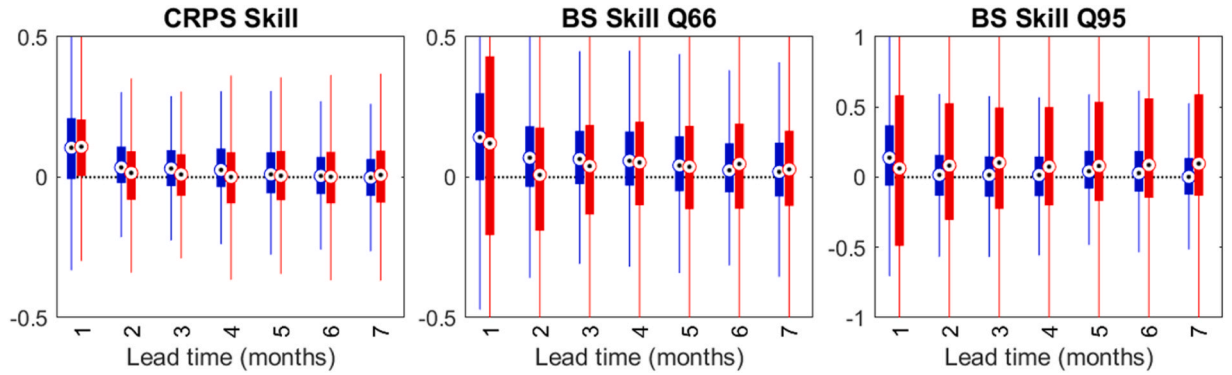

Fig. 12. CRPSS and BSS (Q66 and Q95) for bias-corrected SEAS5-SSF SA according to lead time, considering rivers with drainage area $\geq$ 5000 km^2. Blue presents the Hindcast data results and Red the Forecast results.

3.2. Evaluation of SEAS5-SSF performance in South American rivers

In this section, the performance of bias-corrected SEAS5-SSF from both Hindcast and Forecast experiments is presented. Results are given for large SA rivers (drainage area $>$ 5000 km^2) and are summarized in (1) boxplots, which refer to the entire data periods (i.e., 2007–2016 for hindcast and 2017–2021 for forecast) and (2) maps, which display the spatial distribution of SEAS5-SSF performance according to the season of the year. Only the Hindcast results are presented in map format due to the longer data availability. Spatial maps were produced considering January, April, July and October as target months, i.e., results for July with a 2-month lead time refer to hindcasts issued on June 1st, for example.

In general, Hindcasts results present better performance metrics values than Forecasts. This occurs because not the exact same data is used, and from a slightly different data source, a similar pattern is expected, but with differences in magnitudes. As an example, for the shorter period, the statistical analysis result is more subject to extreme events. The forecast has also less data, and its initialization has fewer observations that were eventually not available when the seasonal meteorological model was operational. This generated the similar pattern between hindcasts and forecasts, but not with the same numerical results.

3.2.1. Ensemble mean metrics

Fig. 7 presents the percentage Bias (relative mean error) and KGE for the bias-corrected SEAS5-SSF. Median Bias ranges from near zero to 5% for Hindcast and 10% for Forecast, while median KGE range from around 0.9–0.7 over the lead times. In the three boxplots, interquartile range increases with lead time, showing that the SEAS5-SSF performance decreases with lead time.

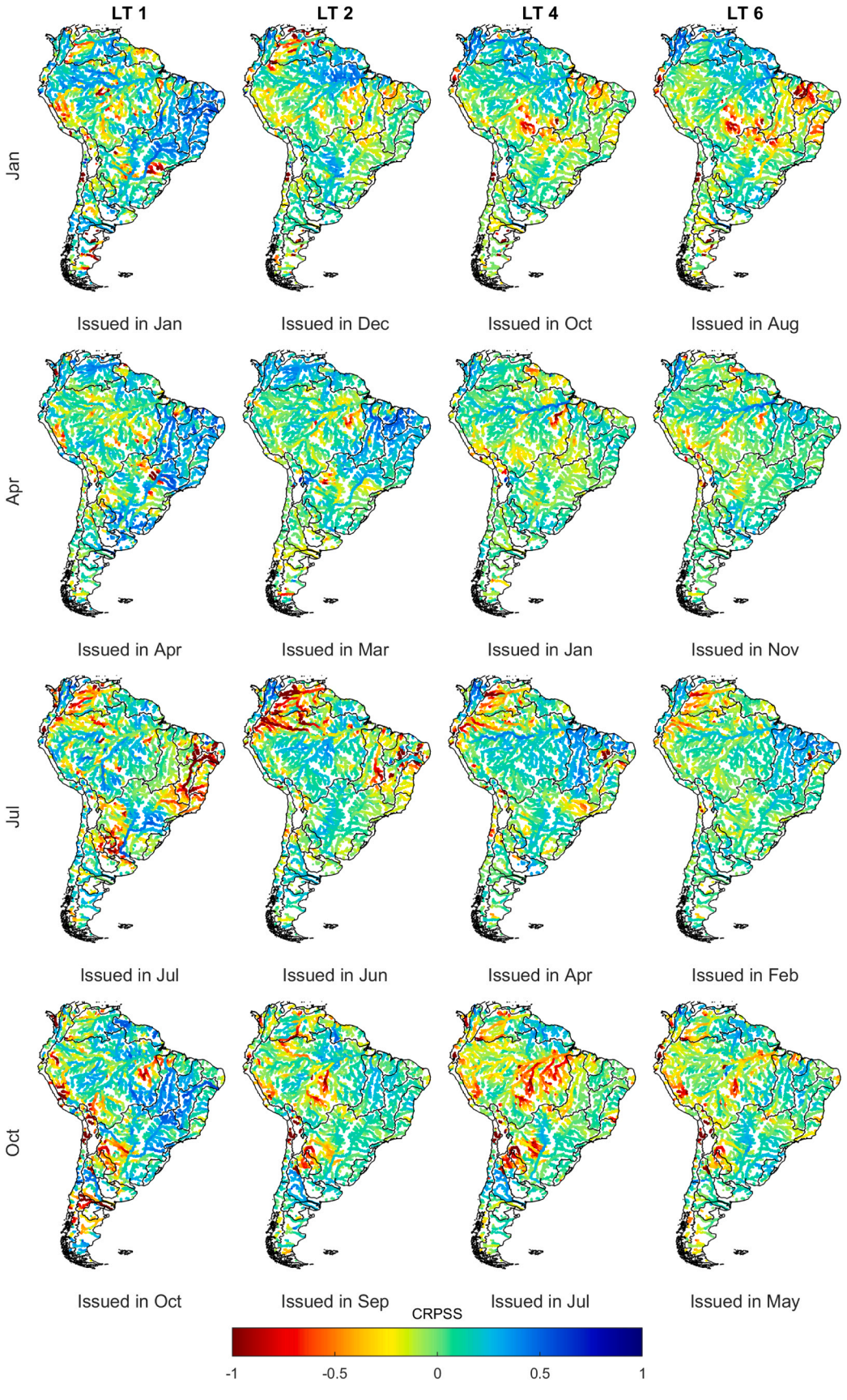

(caption on next page)

Fig. 13. CRPSS for SEAS5-SSF (bias-corrected Hindcasts) relative to the ESP benchmark, according to season and lead time.

Fig. 8 shows the percentage Bias for January, April, July and October for the lead times of one, two, four and six months. Results range from lower bias (yellow) to higher (pink). Streamflow forecast biases are lower in the main river reaches of the great rivers of SA, with a slightly bias increase with lead time. Bias is also very similar for months of different seasons, with only a few regions with higher bias, such as the Northeast and Central Brazil for January forecasts issued with a 4–7-month lead time, north Amazon basin for the forecasts issued in January.

KGE maps (Fig. 9) show that SEAS5-SSF performance decreases with lead time. KGE values are close to unity for the lead time of one month in all seasons, except for rivers near the Andes region. For longer lead times, KGE remains close to unity, mainly in extensive floodplain areas of SA: the Pantanal, the Amazon Delta and Tocantins River Delta.

3.2.2. Full ensemble metrics

Fig. 10 presents the Brier Score (Q66 and Q95 thresholds) for the bias-corrected SEAS5-SSF from Hindcasts. Median BS Q66 range from around 0.03–0.07 and BS Q95 range from around 0.01–0.025 throughout the lead times. In both Fig. 10 boxplots interquartile range increases with lead time, showing unit-catchment general forecast performance decreases with lead time. Q95 Brier Score is lower than BS Q66.

Fig. 11 shows the lower tercile Brier Score for January, April, July and October for the lead time of one, two, four and six months. The assertiveness of low flow occurrence by forecast members is positive related to the precipitation patterns of South America: greater the precipitation, better the brier score (values close to zero). This is the opposite behavior of the CRPS, that shows that greater the precipitation (and greater the rivers), greater are the streamflow errors. In general, the detection of occurrence of low flows by the 25 hindcast members varies spatially within the seasons, but varies very little spatially and in terms of magnitude within the horizons.

Hindcasts Q95 Brier Score maps results are available at the supplementary material.

3.3. Assessment of SEAS5-SSF skill against ESP

The results presented in this section indicate whether the bias-corrected SEAS5-SSF have higher or lower skill than the ESP. Fig. 12 presents the results of CRPSS and BSS (Q66 and Q95) for the Hindcast experiment. In general, the median skill is slightly above zero for c xthe three skill scores, with the lead time of one month showing a higher skill compared with the other lead times. However, the boxplot range indicate that the SEAS5-SSF may outperform the ESP in many rivers while in others do not, presenting skill scores above and below zero for CRPS and BS (Q66 and Q95). Above the 1-month lead time, we observe that all metrics indicate a relatively constant skill over the lead times.

Fig. 13 shows the spatial distribution of CRPSS in SA rivers. Although patterns of skill are not easily noticeable, in some regions the SEAS5-SSF exhibits high (blue) CRPS Skill. SEAS5-SSF issued for the austral summer (January) exhibit consistent positive skill for Northeastern and Southeastern Brazil, more specifically in the Araguaia, São Francisco and upper Paraná River for the first lead time. For longer lead times, positive skill values are lower and are observed near the Amazon River mouth. For April, the Northeast of Brazil and the La Plata Basin showed the higher CRPSS for the lead times of one and two months. The 4th to 6th lead time forecasts to January and April showed high CRPSS only in the Amazon River. In the austral winter (July), SEAS5-SSF presented better skill for the lead times of four and six months (issued in April and February) for the Northeastern Brazil. Streamflow forecasts issued for October, in turn, showed positive CRPSS only for the 1-month lead time.

Seasonal streamflow forecasts issued in February, March and April (Summer/Autumn) seems to have higher skill than those issued in the austral winter months. This may occur because forecasts issued in the Summer (wet season) are predicting discharges for the dry season, and the dry season is consistently easier to predict. Regions such as the Southern Brazil, where precipitation is relatively well distributed throughout the year, consistently showed CRPSS around zero.

Figs. 14 and 15 present the BSS maps for the event thresholds of Q66 and Q95, respectively. The white areas on the maps are infinite and not a number BSS results. These BSS values are originated from the division between the H-EPS Brier Score with the ESP BS when ESP BS is too small (near zero). Besides, these inconclusive BSS results are more frequent in the Q95 results, due to event rarity influence that Q95 commonly represents.

Regarding Fig. 15, we can observe that positive values for BSS do not follow a spatial or temporal pattern. The SEAS5-SSF is skillful in southern Brazil for all horizons and initialization month, except in the Uruguay River regarding October forecasts (all lead times). Besides, for January forecasts, the lower portion of Amazon basin shows high skill for the lead time of one month, whereas in the upper Amazon skill is observed for longer lead times. In other parts of South America, skill is positive in some river reaches of SA during July and October from the 4th to the 7th lead time.

3.4. Analysis of SEAS5-SSF for the Paraná Basin 2020–2021 drought

Fig. 16 shows bias-corrected seasonal streamflow forecasts issued for the Paraná River at the Itaipu Dam in April 2020 and July 2020 at daily timestep (before monthly aggregation) and the Q95 streamflow. By the end of the 2020 and 2021 rainy season, the Brazilian hydropower generation system was under critical regime, with many hydropower plants operating at a fraction of their total capacity (Cuartas et al., 2022). According to Cuartas (2022), the Standardized Precipitation Index (SPI), Standardized Precipitation

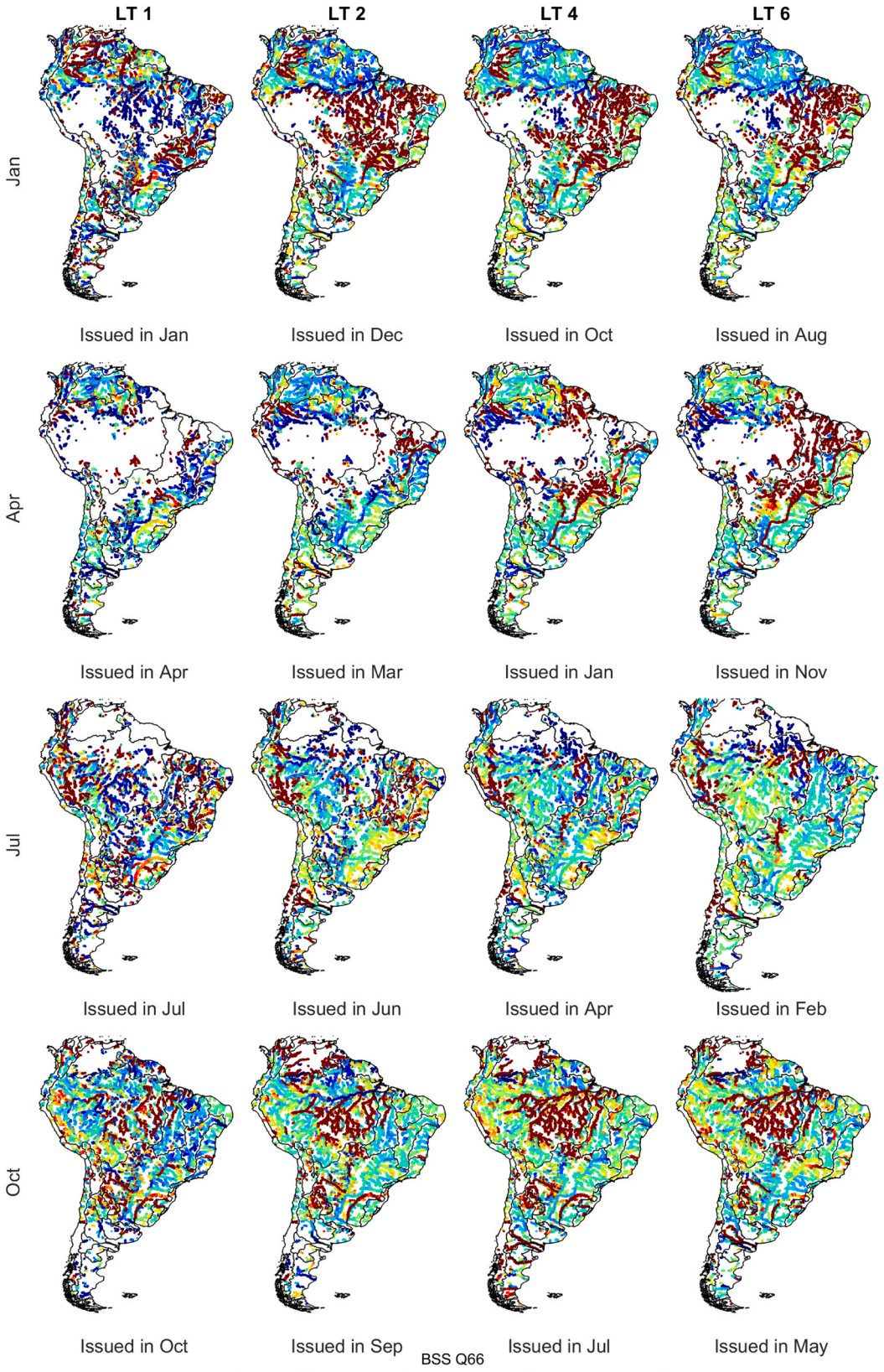

(caption on next page)

Fig. 14. BSS of SEAS5-SSF (bias-corrected Hindcasts) relative to the ESP benchmark, according to season and lead time. The lower tercile of long-term monthly streamflow (Q66) is used as the event threshold.

Evapotranspiration Index (SPEI) and Standardized Streamflow Index (SSFI) values started to decline in 2019, changing from values around zero and reaching − 2 until 2021 (negative values represent streamflow below the climatological average).

At the Itaipu Dam, April is in the transition between the wet and dry seasons (Autumn) and July is the middle of the dry season (Winter). The forecast members predicted future streamflow below Q95, not only in the forecast issued in July, but also in April, a few months before the dry season (Fig. 16). In addition, Fig. 17 presents the ensemble coverage (i.e., the interval between the lower and upper member) and the ensemble mean for lead times of one, two, four and six months. We observe that the predicted streamflow for the 2020 dry season is below Q95 and somewhat below the previous year (winter of 2019). We also observe that the ensemble spread is much smaller for the 1-month lead time (i.e., forecasts issued for day 1–30), which reflects the increase in uncertainty of the forecasts for longer lead times.

Fig. 18 presents the performance metrics of six different seasonal streamflow forecast experiments for the location of the Itaipu Dam. These include the raw and bias-corrected SEAS5-SSF as well as the ESP, considering both forecast and hindcast periods.

The Hindcast experiments present consistently a better performance than those of Forecast for all metrics. Performance decreases with lead time for all metrics and the performance for the 1-month lead time is visibly better. In addition, bias correction improves SEAS5-SSF performance in all metrics and results become closer to the ESP performance (Fig. 18 continuous line is always near the dotted line). It shows not only the added value of bias correction but also the better performance of ESP in comparison to the raw SEAS5-SSF, for this location.

In a closer look at the H-BC results, both CRPSS and BSS are positive for the first lead time, indicating better performance of bias-corrected SEAS5-SSF in predicting low and very low flows than the ESP. However, for the other lead times, the skill is around zero. A relatively good performance of the Brier Score (Q95) can be observed for all forecast experiments at the H-BC results. From the BS formula, one can see that itis a metric that is sensitive to the climatological frequency of the event, in that the rarer an event the easier it is to achieve a good BS without having any real forecast skill.

4. Discussion

The proposed framework based on SEAS5-SSF performance, calculated by ensemble mean metrics (Bias and KGE), indicated better forecast performance for the lead time of one month than the other lead times, with similar behavior for the different seasons of the year. The SEAS5-SSF higher skill in the first lead time is due to the model's dependence on the initial conditions, especially in the bigger basins (e. g. Amazon basin), and near the main river reaches of SA when compared to the river reaches that contribute to them and headwater reaches i.e. Rivers with greater upstream drainage area, commonly showing better predictability due to larger basin size, and thus longer response time (Ghimire et al., 2020; Li et al., 2009; Petry et al., 2022). In smaller and faster basins, such as Uruguay and Iguaçu basins, the skill is due to the higher precipitation prediction performance, attributed to strong ENSO teleconnections (Gubler et al., 2020).

On the lead times greater than one month, the degradation on skill occurs mostly on semi-arid and tropical regions, when we are predicting streamflow for the wet months (e. g. January). These regions present high seasonality (see Fig. 1, c), and such behavior can be seen in the basins São Francisco, headwater reaches of the Paraná Basin and Tocantins/Araguaia. On small basins (most of the headwater reaches), this effect is even stronger, once the initial conditions play a less important role in predictability.

The SEAS5-SSF issued for months typically dry on the tropical region of South America does not lose significant skill on the lead times 2–4 months. This occurs because the model is predicting null precipitation, which is easier, and contrast to the forecasts issued for the wet months on the sub-tropical portion of South America, that presents significantly reduced skill. On the sub-tropical region of SA, even with reduced performance on the lead times greater than 1 month, the SEA5-SSF presents skill, due to the low seasonality of this region (see Fig. 1, c), and so low predictability of the methos ESP. The rainfall observed in South American sub-tropics (excluding the mountains region of the Andes) are typically frontal systems originated on the South Pole and are apparently more predictable by the ECMWF model but less by the ESP.

In the Amazon, the biggest basin on Earth, SEAS5-SSF skill is not always present. The Amazon basin is strongly dependent on the initial conditions (Greuell and Hutjes, 2023; Paiva et al., 2012; Petry et al., 2022), and due to the flat relief of the basin, the water time travel is long. Besides, precipitation regimes and streamflow have significant seasonality (see Fig. 1). These both sources of predictability are also present in the ESP method, explaining the lack of skill of SEAS5-SSF on the Amazon.

Regarding the importance of bias correction, the verification metrics showed added value in removing ECMWF SEAS5 bias to improve streamflow forecast performance: without bias correction, most of the MGB-SA river segments presented negative skill. After bias correction, the median performance of SEAS5-SSF became closer to that of ESP or, in a smaller proportion, outperformed the benchmark. Other authors have already observed the importance of bias correction SEAS5 precipitation forecasts, such as Wang (2019) and Gubler (2020).

5. Conclusions

The results presented comprehends a first assessment of continental-scale seasonal streamflow forecasts in South American (SA) large rivers using a continental hydrologic-hydrodynamic approach.

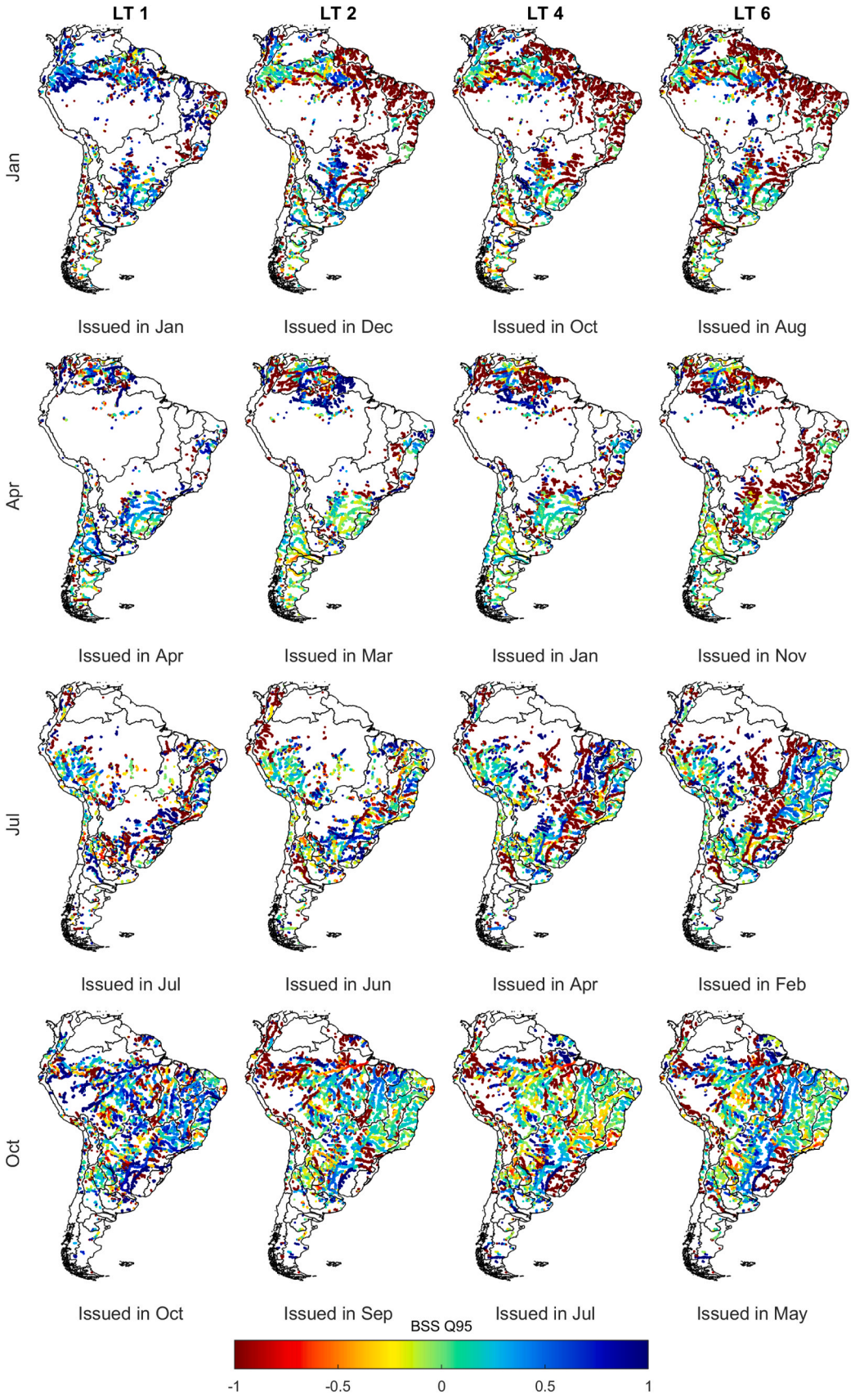

(caption on next page)

Fig. 15. BSS of SEAS5-SSF (bias-corrected Hindcasts) relative to the ESP benchmark, according to season and lead time. The 95th percentile of long-term monthly streamflow (Q95) is used as the event threshold.

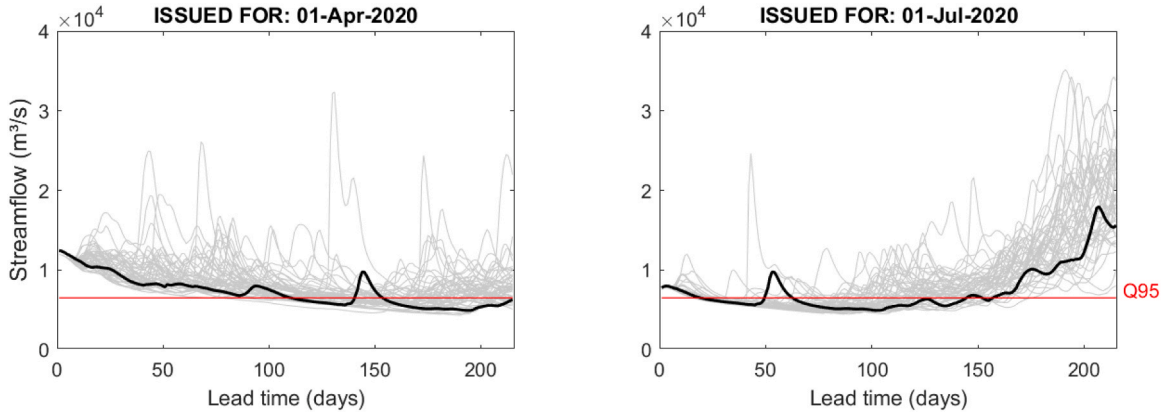

Fig. 16. Bias-corrected SEAS5-SSF issued for April 1st 2020 and July 1st 2020. The SEAS5-SSF ensemble members, MGB-SA reference simulation and Q95 discharge threshold are shown in grey, black and red colors, respectively.

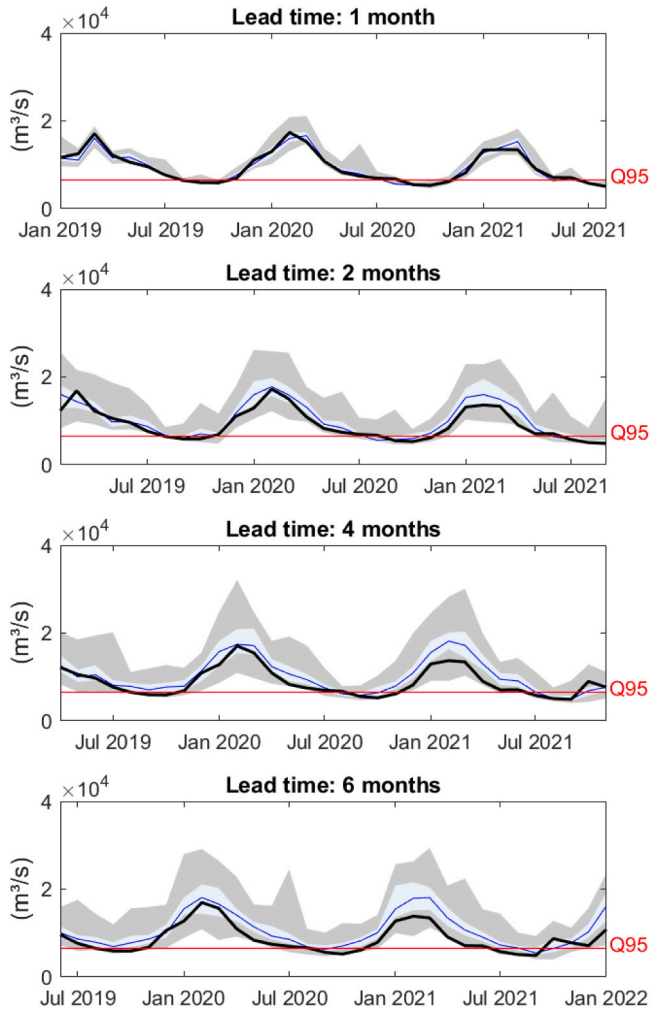

Fig. 17. Bias-corrected SEAS5-SSF issued from January 1st 2019 to January 1st 2022 to the Itaipu Dam. The SEAS5-SSF ensemble members, ensemble mean, MGB-SA reference simulation and Q95 discharge threshold are shown in grey, blue, black and red colors, respectively. The dark gray areas the total ensemble coverage and light grey area 50% prediction interval.

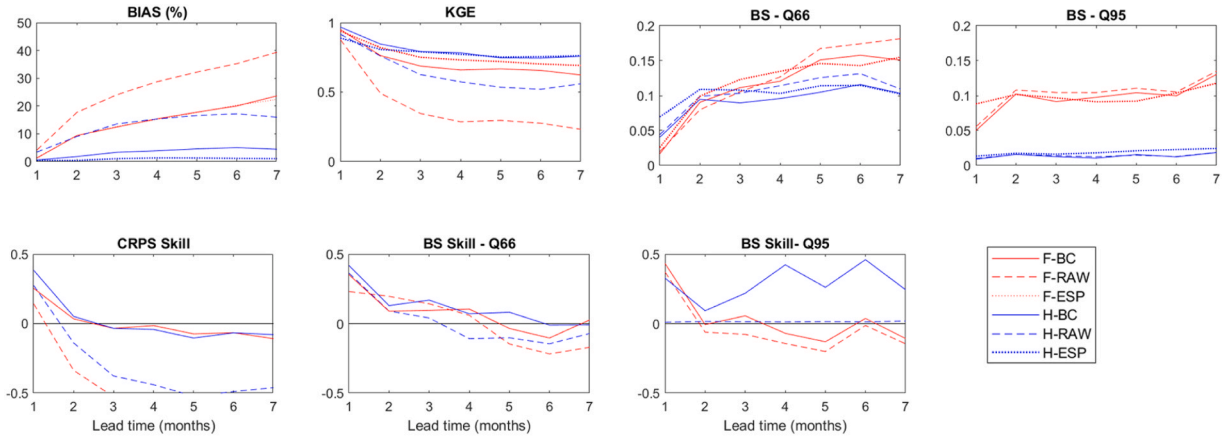

Fig. 18. SEAS5-SSF performance metrics for the Paraná River at the Itaipu Dam. F means Forecast data, H means Hindcast and BC means bias corrected.

We forced the MGB-SA hydrologic-hydrodynamic model with bias-corrected ECMWF SEAS5 predicted precipitation to produce seasonal streamflow forecasts (SEAS5-SSF) and forecast performance was evaluated against a reference simulation run. We also assessed the relative performance of SEAS5-SSF using the Ensemble Streamflow Prediction (ESP) as benchmark, thus providing insights on the added skill of using SEAS5 forecasts for predicting monthly discharges (up to 7 months) in large SA basins.

From the initial hypothesis, we verified that SEAS5-SSF based hydrologic-hydrodynamic forecasts presented the best skill values (for both CRPSS and BSS) on the first month lead time, but ESP was a hard to beat benchmark for SEAS5-SSF in most of South American regions after the 2 months lead-times, mostly in regions with high seasonality, and highly dependent on initial conditions.

Regarding variability associated with the performance of continental forecasts, SEAS5-SSF based forecasts skill varies according to season, initialization month, basin and forecast lead time. In this sense, we understand that our spatial skill results are suited to be used as a tool in the aid to find the best streamflow forecast method (among ESP and H-EPS) for each study area and objective. The rivers where SEAS5-SSF presented the best annual BSS over ESP were the Amazon, Araguaia, Tocantins and Paraná.

The bias correction of SEAS5 predicted precipitation improved the performance of the seasonal streamflow forecasts, frequently turning negative skill results into near null to positive skill.

Future works should address the evaluation of the real skill of the forecasts, including comparison with observed discharges distributed over the continent and especially in the hydroelectric power plant's locations. We expect to investigate techniques on ESP sampling to increase the approach performance based on climatic indicators.

Funding

This work presents part of the results obtained during the project granted by the Brazilian Agency of Electrical Energy (ANEEL) under its Research and Development program Project PD 6491-0503/2018 – "Previsão Hidroclimática com Abrangência no Sistema Interligado Nacional de Energia Elétrica" developed by the Paraná State electric company (COPEL GeT), the Meteorological System of Paraná (SIMEPAR) and the RHAMA Consulting company. The Hydraulic Research Institute (IPH) from the Federal University of Rio Grande do Sul (UFRGS) contribute to part of the project through an agreement with the RHAMA company (IAP-001313).

CRediT authorship contribution statement

Ingrid Petry: Worked on compiling the data, analyzing the results and writing the manuscript. **Fernando Mainardi Fan:** Responsible for the orientation, analysis and discussion of results and writing of the text. **Vinicius Alencar Siqueira**, **Walter Collishonn, Rodrigo Cauduro Dias de Paiva, Erik Quedi and Cléber Henrique de Araújo Gama:** Responsible for analysis and discussion of results and writing of the text. **Reinaldo Silveira, Cassia Silmara Aver Paranhos and Camila Freitas:** Responsible for analysis and discussion of results.

Declaration of Competing Interest

The authors declare that they have no known competing financial interests or personal relationships that could have appeared to influence the work reported in this paper.

Data Availability

Data will be made available on request.

Acknowledgments

The first author thanks Capes for granting a scholarship. The authors are also grateful to the Copernicus Climate Change and Atmosphere Monitoring Services for providing the seasonal forecasts generated by the ECMWF seasonal forecasting systems (SEAS5).

Appendix A. Supporting information

Supplementary data associated with this article can be found in the online version at doi:10.1016/j.ejrh.2023.101487.

References

Alfieri, L., Pappenberger, F., Wetterhall, F., Haiden, T., Richardson, D., Salamon, P., 2014. Evaluation of ensemble streamflow predictions in Europe. J. Hydrol. 517, 913–922. https://doi.org/10.1016/j.jhydrol.2014.06.035.

Alves, M.E.P., Fan, F.M., de Paiva, R.C.D., Siqueira, V.A., Fleischmann, A.S., Brêda, J.P., Laipelt, L., Araújo, A.A., 2022. Assessing the capacity of large-scale hydrologic-hydrodynamic models for mapping flood hazard in southern Brazil. Rev. Bras. De. Recur. Hidr. 27, 1–15. https://doi.org/10.1590/2318-0331.272220220009.

Andreadis, K.M., Schumann, G.J.P., Pavelsky, T., 2013. A simple global river bankfull width and depth database. Water Resour. Res. 49, 7164–7168. https://doi.org/10.1002/wrcr.20440.

Archfield, S.A., Clark, M., Arheimer, B., Hay, L.E., Mcmillan, H., Kiang, J.E., Seibert, J., Hakala, K., Bock, A., Wagener, T., Farmer, W.H., 2015. Accelerating advances in continental domain hydrologic modeling. Water Resour. Manag. 51, 10078–10091. https://doi.org/10.1002/2015WR017498.Received.

Arnal, L., Cloke, H.L., Stephens, E., Wetterhall, F., Prudhomme, C., Neumann, J., Krzeminski, B., Pappenberger, F., 2018. Skilful seasonal forecasts of streamflow over Europe? Hydrol. Earth Syst. Sci. 22, 2057–2072. https://doi.org/10.5194/hess-22-2057-2018.

Bárdossy, A., Pegram, G., 2011. Downscaling precipitation using regional climate models and circulation patterns toward hydrology. Water Resour. Res 47, 1–18. https://doi.org/10.1029/2010WR009689.

Barnston, A.G., Tippett, M.K., L'Heureux, M.L., Li, S., Dewitt, D.G., 2012. Skill of real-time seasonal ENSO model predictions during 2002-11: is our capability increasing? Bull. Am. Meteor. Soc. 93, 631–651. https://doi.org/10.1175/BAMS-D-11-00111.1.

Beck, H.E., Van Dijk, A.I.J.M., Levizzani, V., Schellekens, J., Miralles, D.G., Martens, B., De Roo, A., 2017. MSWEP: 3-hourly 0.25° global gridded precipitation (1979-2015) by merging gauge, satellite, and reanalysis data. Hydrol. Earth Syst. Sci. 21, 589–615. https://doi.org/10.5194/hess-21-589-2017.

Beighley, R.E., Gummadi, V., 2011. Developing channel and floodplain dimensions with limited data: A case study in the Amazon Basin. Earth Surf. Proc. Land. 36, 1059–1071. https://doi.org/10.1002/esp.2132.

Brêda, J.P.L.F., de Paiva, R.C.D., Collischon, W., Bravo, J.M., Siqueira, V.A., Steinke, E.B., 2020. Climate change impacts on South American water balance from a continental-scale hydrological model driven by CMIP5 projections. Clim. Change 159, 503–522. https://doi.org/10.1007/s10584-020-02667-9.

Brier, G.W., 1950. Verification of forecasts expressed in terms of probability. Mon. Weather Rev. 78, 1–3. https://doi.org/10.1016/0016-0032(94)90228-3.

Brown, T.A., 1974. Admissible Scoring Systems for Continuous Distributions.

Buizza, R., Houtekamer, P.L., Toth, Z., Pellerin, G., Wei, M., Zhu, Y., 2005. A Comparison of the ECMWF, MSC, and NCEP global ensemble prediction systems. Mon. Weather Rev. 133, 1076–1097.

Buontempo, C., Thépaut, J., Bergeron, C., 2020. Copernicus climate change service. IOP Conf. Ser.: Earth Environ. Sci. 509 https://doi.org/10.1088/1755-1315/509/1/012005.

Carrão, H., Naumann, G., Dutra, E., Lavaysse, C., Barbosa, P., 2018. Seasonal drought forecasting for Latin America using the ECMWF S4 forecast system. Climate 6, 1–26. https://doi.org/10.3390/cli6020048.

Chiew, F.H.S., Zhou, S.L., McMahon, T.A., 2003. Use of seasonal streamflow forecasts in water resources management. J. Hydrol. (Amst.) 270, 135–144. https://doi.org/10.1016/S0022-1694(02)00292-5.

Cloke, H.L., Pappenberger, F., 2009. Ensemble flood forecasting: a review. J. Hydrol. 375, 613–626. https://doi.org/10.1016/j.jhydrol.2009.06.005.

Collischonn, W., Tucci, C.E.M., Clarke, R.T., Dias, P.L.S., Oliveira, G.S. de, 2005. Previsão Sazonal de Vazão na Bacia do Rio Uruguai 2: Previsão Climática-Hidrológica. Rev. Bras. De. Recur. Hídricos 10, 61–72.

Collischonn, W., Allasia, D., da Silva, B.C., Tucci, C.E.M., 2007. The MGB-IPH model for large-scale rainfall-runoff modelling. Hydrol. Sci. J. 52, 878–895. https://doi.org/10.1623/hysj.52.5.878.

Crochemore, L., Ramos, M.-H., Pappenberger, F., 2016. Bias correcting precipitation forecasts to improve the skill of seasonal streamflow forecasts. Hydrol. Earth Syst. Sci. Discuss. 1–32. https://doi.org/10.5194/hess-2016-78.

Crochemore, L., Cantone, C., Pechlivanidis, I.G., Photiadou, C.S., 2021. How does seasonal forecast performance influence decision-making?; insights from a serious game. Bull. Am. Meteor. Soc. 102, E1682–E1699. https://doi.org/10.1175/BAMS-D-20-0169.1.

Cuartas, L.A., Cunha, A.P.M. do A., Alves, J.A., Parra, L.M.P., Deusdará-Leal, K., Costa, L.C.O., Molina, R.D., Amore, D., Broedel, E., Seluchi, M.E., Cunningham, C., Alvalá, R.C. dos S., Marengo, J.A., 2022. Recent hydrological droughts in Brazil and their impact on hydropower generation. Water 14, 601. https://doi.org/10.3390/w14040601.

Day, G.N., 1985. Extended streamflow forecasting using NWSRFS. J. Water Resour. Plan Manag 111, 157–170. https://doi.org/10.1061/(asce)0733-9496(1985)111:2(157).

De Paiva, L.F.G., Montenegro, S.M., Cataldi, M., 2020. Prediction of monthly flows for Três Marias reservoir (São Francisco river basin using the CFS climate forecast model). Rev. Bras. De. Recur. Hidr. 25, 1–18. https://doi.org/10.1590/2318-0331.252020190067.

Delorit, J., Cristian, E., Ortuya, G., Block, P., 2017. Evaluation of model-based seasonal streamflow and water allocation forecasts for the Elqui Valley. Chile 4711–4725.

Demirel, M.C., Booij, M.J., Hoekstra, A.Y., 2015. The skill of seasonal ensemble low-flow forecasts in the Moselle River for three different hydrological models. Hydrol. Earth Syst. Sci. 19, 275–291. https://doi.org/10.5194/hess-19-275-2015.

Emerton, R., Zsoter, E., Arnal, L., Cloke, H.L., Muraro, D., Prudhomme, C., Stephens, E.M., Salamon, P., Pappenberger, F., 2018. Developing a global operational seasonal hydro-meteorological forecasting system: GloFAS-Seasonal v1.0. Geosci. Model Dev. 11, 3327–3346. https://doi.org/10.5194/gmd-11-3327-2018.

Emerton, R.E., Stephens, E.M., Pappenberger, F., Pagano, T.C., Weerts, A.H., Wood, A.W., Salamon, P., Brown, J.D., Hjerdt, N., Donnelly, C., Baugh, C.A., Cloke, H.L., 2016. Continental and global scale flood forecasting systems. Wiley Interdiscip. Rev.: Water 3, 391–418. https://doi.org/10.1002/wat2.1137.

Fan, F.M., Collischonn, W., Meller, A., Botelho, L.C.M., 2014. Ensemble streamflow forecasting experiments in a tropical basin: The São Francisco river case study. J. Hydrol. (Amst.) 519, 2906–2919. https://doi.org/10.1016/j.jhydrol.2014.04.038.

Fan, F.M., Pontes, P.R.M., Collischonn, W., Buarque, D.C., 2016. Sobre o uso da persistência de previsões determinísticas de vazão para a tomada de decisão. Rev. Bras. De. Meteorol. 31, 218–228. https://doi.org/10.1590/0102-778631220150039.

Fan, F.M., Schwanenberg, D., Collischonn, W., Weerts, A., 2015. Verification of inflow into hydropower reservoirs using ensemble forecasts of the TIGGE database for large scale basins in Brazil. J. Hydrol. Reg. Stud. 4, 196–227. https://doi.org/10.1016/j.ejrh.2015.05.012.

Fan, F.M., Collischonn, W., Quiroz, K.J., Sorribas, M.V., Buarque, D.C., Siqueira, V.A., 2016. Flood forecasting on the Tocantins River using ensemble rainfall forecasts and real-time satellite rainfall estimates. J. Flood Risk Manag 9, 278–288. https://doi.org/10.1111/jfr3.12177.
Ferreira, G.W.S., Reboita, M.S., 2022. A new look into the South America precipitation regimes: observation and forecast. Atmosphere (Basel) 13.
Fleischmann, A., Paiva, R., Collischonn, W., 2019. Can regional to continental river hydrodynamic models be locally relevant? a cross-scale comparison. J. Hydrol. X 3, 100027. https://doi.org/10.1016/j.hydroa.2019.100027.
Fleischmann, A.S., Siqueira, V.A., Wongchuig-Correa, S., Collischonn, W., Paiva, R.C.D.De, 2020. The great 1983 floods in South American large rivers: a continental hydrological modelling approach. Hydrol. Sci. J. 65, 1358–1373. https://doi.org/10.1080/02626667.2020.1747622.
Garreaud, R.D., 2009. The Andes climate and weather. Adv. Geosci. 22, 3–11.
Ghimire, G.R., Jadidoleslam, N., Krajewski, W.F., Tsonis, A.A., 2020. Insights on streamflow predictability across scales using horizontal visibility graph based networks. Front. Water 2, 1–15. https://doi.org/10.3389/frwa.2020.00017.
Greuell, W., Hutjes, R.W.A., 2023. Skill and sources of skill in seasonal streamflow hindcasts for South America made with ECMWF's SEAS5 and VIC. J. Hydrol. (Amst.) 617. https://doi.org/10.1016/j.jhydrol.2022.128806.
Greuell, W., Franssen, W.H.P., Hutjes, R.W.A., 2019. Seasonal streamflow forecasts for Europe - part 2: sources of skill. Hydrol. Earth Syst. Sci. 23, 371–391. https://doi.org/10.5194/hess-23-371-2019.
Gubler, S., Sedlmeier, K., Bhend, J., Avalos, G., Coelho, C.A.S., Escajadillo, Y., Jacques-Coper, M., Martinez, R., Schwierz, C., de Skansi, M., Spirig, C., 2020. Assessment of ECMWF SEAS5 seasonal forecast performance over South America. Weather Forecast 35, 561–584. https://doi.org/10.1175/WAF-D-19-0106.1.
Gupta, H.V., Kling, H., Yilmaz, K.K., Martinez, G.F., 2009. Decomposition of the mean squared error and NSE performance criteria: implications for improving hydrological modelling. J. Hydrol. (Amst.) 377, 80–91. https://doi.org/10.1016/j.jhydrol.2009.08.003.
Gupta, H.V., Perrin, C., Blöschl, G., Montanari, A., Kumar, R., Clark, M., Andréassian, V., 2014. Large-sample hydrology: a need to balance depth with breadth. Hydrol. Earth Syst. Sci. 18, 463–477. https://doi.org/10.5194/hess-18-463-2014.
Harrigan, S., Prudhomme, C., Parry, S., Smith, K., Tanguy, M., 2018. Benchmarking ensemble streamflow prediction skill in the UK. Hydrol. Earth Syst. Sci. 22, 2023–2039. https://doi.org/10.5194/hess-22-2023-2018.
Hersbach, H., 2000. Decomposition of the continuous ranked probability score for ensemble prediction systems. Weather Forecast 15, 559–570. https://doi.org/10.1175/1520-0434(2000)015<0559:DOTCRP>2.0.CO;2.
Johnson, S.J., Stockdale, T.N., Ferranti, L., Balmaseda, M.A., Molteni, F., Magnusson, L., Tietsche, S., Decremer, D., Weisheimer, A., Balsamo, G., Keeley, S.P.E., Mogensen, K., Zuo, H., Monge-Sanz, B.M., 2019a. SEAS5: The new ECMWF seasonal forecast system. Geosci. Model Dev. 12, 1087–1117. https://doi.org/10.5194/gmd-12-1087-2019.
Johnson, S.J., Stockdale, T.N., Ferranti, L., Balmaseda, M.A., Molteni, F., Magnusson, L., Tietsche, S., Decremer, D., Weisheimer, A., Balsamo, G., Keeley, S.P.E., Mogensen, K., Zuo, H., Monge-Sanz, B.M., 2019b. SEAS5: The new ECMWF seasonal forecast system. Geosci. Model Dev. 12, 1087–1117. https://doi.org/10.5194/gmd-12-1087-2019.
Kaune, A., Chowdhury, F., Werner, M., Bennett, J., 2020. The benefit of using an ensemble of seasonal streamflow forecasts in water allocation decisions. Value Using Hydrol. Datasets Water Alloc. Decis.: Earth Obs., Hydrol. Models, Seas. Forecasts 83–113. https://doi.org/10.1201/9781003000389-5.
Kim, H.M., Webster, P.J., Curry, J.A., 2012. Seasonal prediction skill of ECMWF System 4 and NCEP CFSv2 retrospective forecast for the Northern Hemisphere Winter. Clim. Dyn. 39, 2957–2973. https://doi.org/10.1007/s00382-012-1364-6.
Kompor, W., Yoshikawa, S., Kanae, S., 2020. Use of seasonal streamflow forecasts for flood mitigation with adaptive reservoir operation: a case study of the Chao Phraya river basin, Thailand, in 2011. Water (Switz.) 12, 1–19. https://doi.org/10.3390/w12113210.
Koster, R.D., Mahanama, S.P.P., Livneh, B., Lettenmaier, D.P., Reichle, R.H., 2010. Skill in streamflow forecasts derived from large-scale estimates of soil moisture and snow. Nat. Geosci. 3, 613–616. https://doi.org/10.1038/ngeo944.
Lee, D., Ng, J.Y., Galelli, S., Block, P., 2020. Unfolding the relationship between seasonal forecasts skill and value in hydropower production: A global analysis 1–31.
Lehner, B., Döll, P., 2004. Development and validation of a global database of lakes, reservoirs and wetlands. J. Hydrol. 296, 1–22. https://doi.org/10.1016/j.jhydrol.2004.03.028.
Li, H., Luo, L., Wood, E.F., Schaake, J., 2009. The role of initial conditions and forcing uncertainties in seasonal hydrologic forecasting. J. Geophys. Res. Atmospheres 114, 1–10. https://doi.org/10.1029/2008JD010969.
Liu, L., Wu, Y., Zhang, P., Zhai, J., Zhang, L., Xiao, C., 2021. Predictability of seasonal streamflow forecasting based on CSM: Case studies of top three largest rivers in China. Water (Switz.) 13, 1–14. https://doi.org/10.3390/w13020162.
Lopes, R., Fan, F.M., Rógenes, P., Pontes, M., Siqueira, V.A., Collischonn, W., Marques, M., 2018. A first integrated modelling of a river-lagoon large-scale hydrological system for forecasting purposes. J. Hydrol. (Amst. 565, 177–196. https://doi.org/10.1016/j.jhydrol.2018.08.011.
Lorenz, E.N., 1993. Our Chaotic Weather. in: The Essence of Chaos. Seattle, pp. 88–121. https://doi.org/10.4324/9780203214589_chapter_3.
Mahanama, S., Livneh, B., Koster, R., Lettenmaier, D., Reichle, R., 2012. Soil moisture, snow, and seasonal streamflow forecasts in the United States. Am. Meteorol. Soc. 189–203. https://doi.org/10.1175/JHM-D-11-046.1.
Najafi, M.R., Moradkhani, H., Asce, F., 2015. Towards Ensemble Combination of Seasonal Streamflow Forecasts Ensemble Combination of Seasonal Streamflow Forecasts. https://doi.org/⟨10.1061/(ASCE)HE.1943–5584.0001250⟩.
New, M., Lister, D., Hulme, M., Makin, I., 2002. A high-resolution data set of surface climate over global land areas. Clim. Res 21, 1–25. https://doi.org/10.3354/cr021001.
O'Loughlin, F.E., Paiva, R.C.D., Durand, M., Alsdorf, D.E., Bates, P.D., 2016. A multi-sensor approach towards a global vegetation corrected SRTMDEM product. Remote Sens. Environ. 182, 49–59. https://doi.org/10.1016/j.rse.2016.04.018.
Paiva, R.C.D., Collischonn, W., Bonnet, M.P., De Gonçalves, L.G.G., 2012. On the sources of hydrological prediction uncertainty in the Amazon. Hydrol. Earth Syst. Sci. 16, 3127–3137. https://doi.org/10.5194/hess-16-3127-2012.
Paiva, R.C.D., Collischonn, W., Bonnet, M., Gonc, L.G.G.De, 2013. Assimilating in situ and radar altimetry data into a large-scale hydrologic-hydrodynamic model for streamflow forecast in the Amazon. Hydrol. Earth Syst. Sci. 2929–2946. https://doi.org/10.5194/hess-17-2929-2013.
Pappenberger, F., Ramos, M.H., Cloke, H.L., Wetterhall, F., Alfieri, L., Bogner, K., Mueller, A., Salamon, P., 2015. How do I know if my forecasts are better? Using benchmarks in hydrological ensemble prediction. J. Hydrol. (Amst.) 522, 697–713. https://doi.org/10.1016/j.jhydrol.2015.01.024.
Pechlivanidis, I.G., Arheimer, B., 2015. Large-scale hydrological modelling by using modified PUB recommendations: The India-HYPE case. Hydrol. Earth Syst. Sci. 19, 4559–4579. https://doi.org/10.5194/hess-19-4559-2015.
Pechlivanidis, I.G., Crochemore, L., Rosberg, J., Bosshard, T., 2020. What are the key drivers controlling the quality of seasonal streamflow forecasts? Water Resour. Res 56, 1–19. https://doi.org/10.1029/2019wr026987.
Peñuela, A., Hutton, C., Pianosi, F., 2020. Assessing the value of seasonal hydrological forecasts for improving water resource management: Insights from a pilot application in the UK. Hydrol. Earth Syst. Sci. 24, 6059–6073. https://doi.org/10.5194/hess-24-6059-2020.
Petry, I., Fan, F.M., Siqueira, V.A., Freitas, C., Paranhos, C.S.A., 2021. Analysis of seasonal streamflow forecasts based on the ecmwf seas5 system for the 1983 South American historical flood at Itaipu dam. In: ABRhidro (Ed.), XXIV Simpósio Brasileiro de Recursos Hídricos. Belo Horizonte.
Petry, I., Fan, F.M., Siqueira, V.A., Paiva, R., Petry, I., Fan, F.M., 2022. Predictability of daily streamflow for the great rivers of South America based on a simple metric a simple metric. Hydrol. Sci. J. 00, 1–15. https://doi.org/10.1080/02626667.2022.2139620.
Piani, C., Haerter, J.O., Coppola, E., 2010. Statistical bias correction for daily precipitation in regional climate models over Europe. Theor. Appl. Clim. 99, 187–192. https://doi.org/10.1007/s00704-009-0134-9.
Pontes, P.R.M., Collischonn, W., Fan, F.M., Paiva, R.C.D., Buarque, D.C., 2015. Hydrologic and hydraulic large-scale modeling with inertial flow routing. Water Clim.: Model. Large Basins 3, 1–84.
Pontes, P.R.M., Fan, F.M., Fleischmann, A.S., de Paiva, R.C.D., Buarque, D.C., Siqueira, V.A., Jardim, P.F., Sorribas, M.V., Collischonn, W., 2017. MGB-IPH model for hydrological and hydraulic simulation of large floodplain river systems coupled with open source GIS. Environ. Model. Softw. 94, 1–20. https://doi.org/10.1016/j.envsoft.2017.03.029.

Quedi, E.S., Fan, F.M., 2020. Sub seasonal streamflow forecast assessment at large-scale basins. J. Hydrol. (Amst.) 584, 124635. https://doi.org/10.1016/j.jhydrol.2020.124635.

Shukla, J., 1998. Predictability in the midst of chaos: a scientific basis for climate forecasting. Science (1979) 282, 728–731. https://doi.org/10.1126/science.282.5389.728.

Siqueira, V.A., Collischonn, W., Fan, F.M., Chou, S.C., 2016. Ensemble flood forecasting based on operational forecasts of the regional Eta EPS in the Taquari-Antas basin. Rev. Bras. De. Recur. Hidr. 21, 587–602. https://doi.org/10.1590/2318-0331.011616004.

Siqueira, V.A., Paiva, R.C.D., Fleischmann, A.S., Fan, F.M., Ruhoff, A.L., Pontes, P.R.M., Paris, A., Calmant, S., Collischonn, W., Anderson, L., Pontes, P.R.M., Paris, A., Calmant, S., Collischonn, W., 2018. Toward continental hydrologic – hydrodynamic modeling in South America. Hydrol. Earth Syst. Sci. 22, 4815–4842.

Siqueira, V.A., Fan, F.M., Paiva, R.C.D. de, Ramos, M.H., Collischonn, W., Alencar, V., Mainardi, F., Cauduro, R., Paiva, D.De, Pesquisas, I.De, Iph, H., Alegre, P., 2020. Potential skill of continental-scale, medium-range ensemble streamflow forecasts for flood prediction in South America. J. Hydrol. 590, 125430 https://doi.org/10.1016/j.jhydrol.2020.125430.

Siqueira, V.A., Weerts, A., Klein, B., Fan, F.M., Paiva, R.C.D. de, Collischonn, W., 2021. Postprocessing continental-scale, medium-range ensemble streamflow forecasts in South America using Ensemble Model Output Statistics and Ensemble Copula Coupling. J. Hydrol. (Amst.) 600, 126520. https://doi.org/10.1016/j.jhydrol.2021.126520.

Skofronick-Jackson, G., Petersen, W.A., Berg, W., Kidd, C., Stocker, E.F., Kirschbaum, D.B., Kakar, R., Braun, S.A., Huffman, G.J., Iguchi, T., Kirstetter, P.E., Kummerow, C., Meneghini, R., Oki, R., Olson, W.S., Takayabu, Y.N., Furukawa, K., Wilheit, T., 2017. The global precipitation measurement (GPM) mission for science and Society. Bull. Am. Meteor. Soc. 98, 1679–1695. https://doi.org/10.1175/BAMS-D-15-00306.1.

Sutanto, S.J., Wetterhall, F., Van Lanen, H.A.J., 2020. Hydrological drought forecasts outperform meteorological drought forecasts. Environ. Res. Lett. 15 https://doi.org/10.1088/1748-9326/ab8b13.

Troin, M., Arsenault, R., Wood, A.W., Brissette, F., Martel, J.-L.L., 2021. Generating ensemble streamflow forecasts: a review of methods and approaches over the past 40 years Accepted. Water Resour. Res. https://doi.org/10.1029/2020WR028392.

Tucci, C.E.M., Clarke, R.T., Collischonn, W., Da Silva Dias, P.L., De Oliveira, G.S., 2003. Long-term flow forecasts based on climate and hydrologic modeling: Uruguay River basin. Water Resour. Res 39, 1–11. https://doi.org/10.1029/2003WR002074.

Van Dijk, A.I.J.M., Peña-Arancibia, J.L., Wood, E.F., Sheffield, J., Beck, H.E., 2013. Global analysis of seasonal streamflow predictability using an ensemble prediction system and observations from 6192 small catchments worldwide. Water Resour. Res 49, 2729–2746. https://doi.org/10.1002/wrcr.20251.

Van Hateren, T.C., Sutanto, S.J., Van Lanen, H.A.J., 2019. Evaluating skill and robustness of seasonal meteorological and hydrological drought forecasts at the catchment scale – Case Catalonia (Spain). Environ. Int 133, 105206. https://doi.org/10.1016/j.envint.2019.105206.

Wang, Q.J., Shao, Y., Song, Y., Schepen, A., Robertson, D.E., Ryu, D., Pappenberger, F., 2019. An evaluation of ECMWF SEAS5 seasonal climate forecasts for Australia using a new forecast calibration algorithm. Environ. Model. Softw. 122, 104550 https://doi.org/10.1016/j.envsoft.2019.104550.

Weisheimer, A., Befort, D.J., MacLeod, D., Palmer, T., O'Reilly, C., Strømmen, K., 2020. Seasonal Forecasts of the Twentieth Century. Bull. Am. Meteor. Soc. 101, E1413–E1426. https://doi.org/10.1175/bams-d-19-0019.1.

WMO, 2008. Hydrological forecasting, in: guide to hydrological practices: Vol II: hydrology - management of water resources and application of hydrological practices. World Meteorological Organisation (WMO), Genova, Switzerland, pp. II.7-1–II.7-34.

Wood, A.W., Lettenmaier, D.P., 2008. An ensemble approach for attribution of hydrologic prediction uncertainty. Geophys Res Lett. 35, 1–5. https://doi.org/10.1029/2008GL034648.

Yamazaki, D., Kanae, S., Kim, H., Oki, T., 2011. A physically based description of floodplain inundation dynamics in a global river routing model. Water Resour. Res 47. https://doi.org/10.1029/2010WR009726.

Yamazaki, D., De Almeida, G.A.M., Bates, P.D., 2013. Improving computational efficiency in global river models by implementing the local inertial flow equation and a vector-based river network map. Water Resour. Res 49, 7221–7235. https://doi.org/10.1002/wrcr.20552.

Yossef, N.C., Winsemius, H., Weerts, A., Van Beek, R., Bierkens, M.F.P., 2013. Skill of a global seasonal streamflow forecasting system, relative roles of initial conditions and meteorological forcing. Water Resour. Res 49, 4687–4699. https://doi.org/10.1002/wrcr.20350.

Yuan, X., 2016. An experimental seasonal hydrological forecasting system over the Yellow River basin - part 2: The added value from climate forecast models. Hydrol. Earth Syst. Sci. 20, 2453–2466. https://doi.org/10.5194/hess-20-2453-2016.

Yuan, X., Roundy, J.K., Wood, E.F., Sheffield, J., 2015. Seasonal forecasting of global hydrologic extremes: system development and evaluation over GEWEX basins. Bull. Am. Meteor. Soc. 96, 1895–1912. https://doi.org/10.1175/BAMS-D-14-00003.1.